Linear-Phase Perfect Reconstruction Filter Bank: Lattice Structure, Design, and Application in Image Coding

Trac D. Tran, Ricardo L. de Queiroz, *Senior Member, IEEE,* and Truong Q. Nguyen, *Senior Member, IEEE*

***Abstract*—A lattice structure for an M-channel linear-phase perfect reconstruction filter bank (LPPRFB) based on the singular value decomposition (SVD) is introduced. The lattice can be proven to use a minimal number of delay elements and to completely span a large class of LPPRFB's: All analysis and synthesis filters have the same FIR length, sharing the same center of symmetry. The lattice also structurally enforces both linear-phase and perfect reconstruction properties, is capable of providing fast and efficient implementation, and avoids the costly matrix inversion problem in the optimization process. From a block transform perspective, the new lattice can be viewed as representing a family of generalized lapped biorthogonal transform (GLBT) with an arbitrary number of channels M and arbitrarily large overlap. The relaxation of the orthogonal constraint allows the GLBT to have significantly different analysis and synthesis basis functions, which can then be tailored appropriately to fit a particular application. Several design examples are presented along with a high-performance GLBT-based progressive image coder to demonstrate the potential of the new transforms.**

I. Introduction

THERE HAS been a tremendous growth in the field of filter banks (FB's) and multirate systems in the last 15 years. These systems provide new and effective ways to represent signals for processing, understanding, and compression purposes. Filter banks find applications in virtually every signal processing field [1]–[3]. Obviously, of extreme importance is the ability to design a filter bank that can fully exploit the properties and nature of a particular class of signals or applications.

In this paper, we consider the discrete-time maximally decimated M-channel uniform filter bank as depicted in Fig. 1(a). At the analysis stage, the input signal $x[n]$ is passed through a bank of M analysis filters $H_i(z)$, each of which preserves a frequency band of uniform bandwidth π/M. These M filtered signals are then decimated by M to preserve the system's overall sampling rate. The resulting subband signals can be coded, processed, and/or transmitted independently or jointly. At the synthesis stage, the subbands are combined by a set of upsamplers and M synthesis filters $F_i(z)$ to form the reconstructed signal $\hat{x}[n]$. Assuming that there is no information loss at the processing stage, filter banks that yield the output $\hat{x}[n]$ as a purely delayed version of the input $x[n]$, i.e., $\hat{x}[n] = x[n - n_0]$, are called perfect reconstruction (PR) filter banks. The PR property is highly desirable since it provides a lossless signal representation, and it simplifies the error analysis significantly.

In numerous applications, especially image processing, it is also crucial that all analysis and synthesis filters have linear phase (LP). Besides the elimination of the phase distortion, LP systems allow us to use simple symmetric extension methods to accurately handle the boundaries of finite-length signals. Furthermore, the LP property can be exploited, leading to faster and more efficient FB implementation. From this point on, all of the FB in discussion are LP perfect reconstruction filter bank (LPPRFB). For various other practical purposes, only causal, FIR, and real-coefficient systems are under consideration.

The M-channel filter bank in Fig. 1(a) can also be represented in terms of its polyphase matrices as shown in Fig. 1(b), where $\boldsymbol{E}(z)$ is the analysis bank's polyphase matrix, and $\boldsymbol{R}(z)$ is the synthesis bank's polyphase matrix. Note that both $\boldsymbol{E}(z)$ and $\boldsymbol{R}(z)$ are $M \times M$ matrices whose elements are polynomials in z [1]. Now, if $\boldsymbol{E}(z)$ is invertible with minimum-phase determinant (stable inverse), we can obtain PR by simply choosing $\boldsymbol{R}(z) = \boldsymbol{E}^{-1}(z)$. In other words, any choice of $\boldsymbol{R}(z)$ and $\boldsymbol{E}(z)$ that satisfies

$$\boldsymbol{R}(z)\boldsymbol{E}(z) = z^{-l}\boldsymbol{I}, \qquad l \geq 0 \tag{1}$$

yields PR. Since we are only interested in FIR FB, the determinants of both polyphase matrices need to be monomials [1] as well:

$$|\boldsymbol{R}(z)| = z^{-m} \quad \text{and} \quad |\boldsymbol{E}(z)| = z^{-n} \qquad m, n \text{ integers.} \tag{2}$$

A popular choice of $\boldsymbol{R}(z)$ in several previous works [4]–[7] is

$$\boldsymbol{R}(z) = z^{-K}\boldsymbol{E}^{T}\left(z^{-1}\right) \tag{3}$$

where K is the order of a properly designed $\boldsymbol{E}(z)$. This leads to *paraunitary* or *orthogonal* systems. In the case where $\boldsymbol{E}(z)$

Manuscript received May 7, 1998; revised June 20, 1999. This work was supported in part by the National Science Foundation under Grant MIP-9501589. The associate editor coordinating the review of this paper and approving it for publication was Dr. Sergios Theodoridis.

T. D. Tran was with the Department of Electrical and Computer Engineering, University of Wisconsin, Madison, WI 53706 USA. He is now with the Department of Electrical and Computer Engineering, The Johns Hopkins University, Baltimore, MD 21218 USA (e-mail: ttran@ece.jhu.edu).

R. L. de Queiroz is with Corporate Research and Technology, Xerox Corporation, Webster, NY 14580 USA (e-mail: queiroz@wrc.xerox.com).

T. Q. Nguyen is with the Electrical and Computer Engineering Department, Boston University, MA 02215 USA (e-mail: nguyent@bu.edu).

Publisher Item Identifier S 1053-587X(00)00106-9.

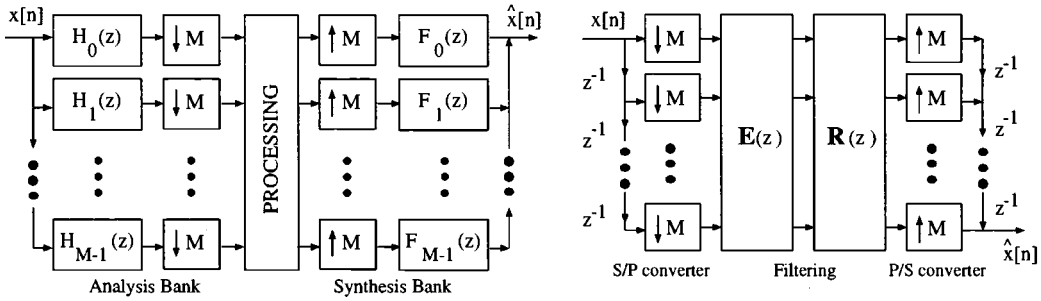

Fig. 1. M-channel uniform-band maximally decimated filter bank. (a) Conventional representation. (b) Polyphase representation.

may not be paraunitary but (1) still holds, the FB is said to be *biorthogonal*.

A. Previous Works

There have been numerous works on the theory, design, and implementation of FIR LPPRFB [1]–[3]. Most deals with two-channel biorthogonal systems [8]–[10] for which all solutions have been found. A Type A system has even-length filters with different symmetry polarity (where one is symmetric and the other antisymmetric). A Type B system has odd-length filters with the same symmetry polarity (both symmetric) [11]. On the other hand, there are still many open problems in M-channel cases. First of all, when $M > 2$, there is no simple spectral factorization method that has worked well in practice for two-channel FB design [2]. We have to rely on other approaches such as lattice structure parameterization [4]–[7], time-domain optimization [12]–[14], and cosine modulation [15]. The most attractive amongst these is the lattice structure approach based on the factorization of the polyphase matrices $\boldsymbol{E}(z)$ and $\boldsymbol{R}(z)$. The lattice structure offers fast implementation with a minimal number of delay elements, retains both LP and PR properties regardless of lattice coefficient quantization, and, if it is general enough, covers a complete class of FB with certain desired properties. Complete and minimal two-channel LP PR lattice structures have been reported in [8]. M-channel lattices have been found for the more restricted paraunitary case [4], resulting in the generalized lapped orthogonal transform (GenLOT) [5], [6]. No general lattice has been reported for the biorthogonal case. Only several particular solutions were proposed thus far. Chan replaced some orthogonal matrices in [5] by cascades of invertible block diagonal matrices [16]. Malvar suggested the lapped biorthogonal transform (LBT) by introducing a $\sqrt{2}$ scaling of the first antisymmetric basis function of the DCT, which serves as the initial block of the original LOT structure [17], [18]. Although this elegant solution leads to fast-computable transforms that are highly desirable in practice, it is certainly not the general solution. This paper is indeed a direct inspirational product of Malvar's work in [18].

As previously mentioned, an M-channel LPPRFB can be implemented as a lapped transform (LT), as demonstrated in Fig. 2 [19]. In the one-dimensional (1-D) direct implementation, the input signal can be blocked into sequences of length $L = KM$ and overlapped by $M(K-1)$ samples with adjacent sequences. The M columns of the transform coefficient matrix $\boldsymbol{P}$ hold the impulse responses of the analysis filters $h_i[n]$. The resulting M subbands $X_i[n]$ can then be quantized, coded, and transmitted to the decoder, where the inverse transform is performed to reconstruct the original signal $x[n]$. The LT provides an elegant solution to the elimination of annoying blocking artifacts in traditional block-transform image coders at a reasonable cost—in both system memory requirement and transform speed. The LT outperforms the popular nonoverlapped discrete cosine transform (DCT) [20] on two counts: i) From the analysis viewpoint, it takes into account interblock correlation, hence, providing better energy compaction, and ii) from the synthesis viewpoint, its basis functions decay asymptotically to zero at the ends, reducing blocking discontinuities drastically. The original LOT and its generalized version are LPPUFB's and, as a result, have identical analysis and synthesis banks [1], [19]. The relaxation of the orthogonal constraint gives the new class of LT's much more flexibility, especially in image coding application. In the analysis bank, a lot of emphasis can be placed on energy compaction, whereas in the synthesis bank, the smoothness property of the filters can be concentrated on to improve the visual quality of the reconstructed images.

B. Outline

The outline of the paper is as follows. Taking a step toward unifying the field of M-channel LPPRFB design, we first introduce in Section II a general and unique structure that propagates the LP and PR properties. Section III discusses the particular solution for the even-channel case where the resulting lattice is proven to be complete and minimal. In the LT language, the structure can be interpreted as a robust and efficient characterization of the generalized lapped biorthogonal transform (GLBT). The odd-channel solution is presented in Section IV. Next, Section V introduces the novel parameterization of invertible coefficient matrices by the singular value decomposition (SVD) that allows robust characterization of biorthogonality and avoids the costly matrix inversion in the optimization process. In Section VI, several design examples based on unconstrained nonlinear optimization of the lattice coefficients are presented along with an image coding example illustrating the new LT family's potential. The GLBT-based embedded coder consistently outperforms the wavelet-based SPIHT coder [21] by a large margin. The improvement in PSNR can be up to an astounding 2.6 dB. Finally, Section VII draws up the final conclusions.

C. Notation

Notation-wise, vectors are denoted by boldfaced lowercase characters, whereas matrices are denoted by boldfaced uppercase characters. If their sizes are not clear from context, subscripts are provided. $\boldsymbol{A}^T$, $\boldsymbol{A}^{-1}$, $\mathrm{tr}(\boldsymbol{A})$, $|\boldsymbol{A}|$, and $\rho(\boldsymbol{A})$ denote, respectively, the transpose, the inverse, the trace, the determinant, and the rank of the matrix $\boldsymbol{A}$. If $\boldsymbol{A}(z)$ has an inverse and its determinant is a pure delay as defined in (2), $\boldsymbol{A}(z)$ is called FIR invertible or having FIR inverses. The symbols $h_i[n]$, $H_i(z)$, and $H_i(e^{j\omega})$ stand for the ith filter's impulse response, its associated z-transform, and its Fourier transform, respectively. Several special matrices have reserved symbols:

- $\boldsymbol{I}$ identity matrix;
- $\boldsymbol{J}$ reversal matrix;
- $\boldsymbol{0}$ null matrix
- $\boldsymbol{D}$ diagonal matrix whose entry is $+1$ when the corresponding filter is symmetric and -1 when the corresponding filter is antisymmetric.

M and L are reserved for the number of channels and the filter length. For abbreviations, we use LP, PR, PU, LT, and FB to denote *linear phase, perfect reconstruction, paraunitary, lapped transform,* and *filter bank*. The terms LPPRFB and GLBT are used interchangeably.

II. General LP-Propagating Structure

A. Problem Formulation

Throughout this paper, the class of M-channel FB's under investigation possesses all of the following characteristics.

i) The FB has perfect reconstruction as in (1).
ii) All filters (both analysis and synthesis) are FIR as in (2).
iii) All filters have the same length $L = KM$, where K is a positive integer, i.e., $\boldsymbol{E}(z)$ and $\boldsymbol{R}(z)$ have the same order.
iv) All analysis and synthesis filters have real coefficients and LP, i.e., they are either symmetric $h[n] = h[L-1-n]$ or antisymmetric $h[n] = -h[L-1-n]$.

For this class of LPPRFB, the problem of permissible conditions on the filter length and symmetry polarity has been solved in [6], [22], and [23]. Their fundamental results are summarized in Table I. These necessary conditions for LPPR systems are extremely helpful in restricting the search space of possible solutions, and they also play a key role in the development of general lattice structures presented in the next sections.

B. General Structure

The essential concept of the lattice structure can be best illustrated in Fig. 3. Suppose we are given a set of filters $\{H_{F,i}(z)\}$ with the associated polyphase matrix $\boldsymbol{F}(z)$ satisfying a certain set of desired properties. We would like to design a low-ordered structure $\boldsymbol{G}(z)$ to translate $\{H_{F,i}(z)\}$ into another set of filters $\{H_{E,i}(z)\}$ of higher order represented by the new polyphase matrix $\boldsymbol{E}(z) = \boldsymbol{G}(z)\boldsymbol{F}(z)$ in such a way that $\{H_{E,i}(z)\}$ still possesses the same set of desired properties as $\{H_{F,i}(z)\}$. The following theorem introduces a general structure for $\boldsymbol{G}(z)$, where the propagating properties are chosen to be LP and PR.

Theorem I: Suppose that there exists an M-channel FIR LPPRFB with all analysis and synthesis filters of length $L = KM$

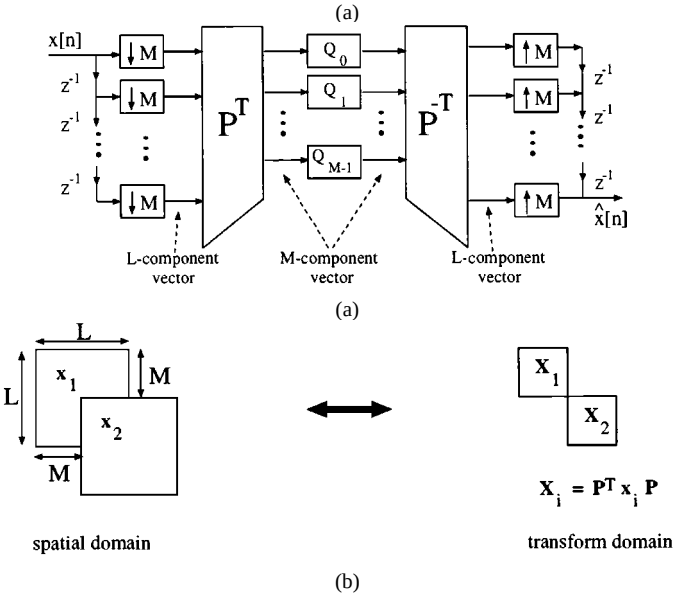

Fig. 2. M-channel LPPRFB as an LT. (a) Direct implementation in 1-D. (b) Illustration in 2-D.

TABLE I
POSSIBLE SOLUTIONS FOR M-CHANNEL LPPRFB WITH FILTER LENGTHS $L_i = K_iM + \beta$

Case	*Symmetry Polarity Condition*	*Length Condition*	*Sum of Lengths*
M even, β even	$\frac{M}{2}$ S & $\frac{M}{2}$ A	$\sum K_i$ even	$2mM$
M even, β odd	$(\frac{M}{2}+1)$ S & $(\frac{M}{2}-1)$ A	$\sum K_i$ odd	$2mM$
M odd, β even	$(\frac{M+1}{2})$ S & $(\frac{M-1}{2})$ A	$\sum K_i$ odd	$(2m+1)M$
M odd, β odd	$(\frac{M+1}{2})$ S & $(\frac{M-1}{2})$ A	$\sum K_i$ even	$(2m+1)M$

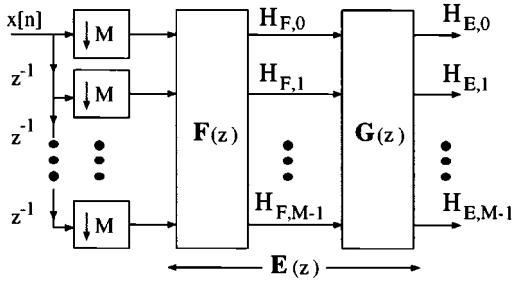

Fig. 3. Stage of the lattice structure.

with the associated order-$(K-1)$ polyphase matrix $\boldsymbol{F}(z)$. Define the order-$(K+N-1)$ polyphase matrix $\boldsymbol{E}(z) \triangleq \boldsymbol{G}(z)\boldsymbol{F}(z)$, where the propagating structure is the all-zero $\boldsymbol{G}(z)$ of order N, i.e., $\boldsymbol{G}(z) = \sum_{i=0}^{N} \boldsymbol{A}_i z^{-i}$. Then, $\boldsymbol{E}(z)$ has LP and PR if and only if

1) $\boldsymbol{G}(z)$ is FIR invertible;
2) $\boldsymbol{G}(z)$ takes the form $\boldsymbol{G}(z) = z^{-N}\boldsymbol{D}\boldsymbol{G}(z^{-1})\boldsymbol{D}$;
3) $\boldsymbol{A}_i = \boldsymbol{D}\boldsymbol{A}_{N-i}\boldsymbol{D}$.

Proof: First, $\boldsymbol{E}(z) = \boldsymbol{G}(z)\boldsymbol{F}(z)$; hence, $|\boldsymbol{E}(z)| = |\boldsymbol{G}(z)|\,|\boldsymbol{F}(z)|$, and $\boldsymbol{E}^{-1}(z) = \boldsymbol{F}^{-1}(z)\boldsymbol{G}^{-1}(z)$. Since $\boldsymbol{F}(z)$ is FIR invertible, it is clear that $\boldsymbol{E}^{-1}(z)$ exists and is FIR if and only if $\boldsymbol{G}(z)$ is FIR invertible. Next, $\boldsymbol{F}(z)$ represents a LPFB; therefore, $\boldsymbol{F}(z)$ and its associated synthesis polyphase matrix $\boldsymbol{R}(z)$ satisfy the LP property [4], [6]

$$\boldsymbol{F}(z) = z^{-(K-1)}\boldsymbol{D}\boldsymbol{F}\left(z^{-1}\right)\boldsymbol{J} \quad \text{(analysis)} \tag{4}$$

$$\boldsymbol{R}(z) = z^{-(K-1)}\boldsymbol{J}\boldsymbol{R}\left(z^{-1}\right)\boldsymbol{D} \quad \text{(synthesis)} \tag{5}$$

where $\boldsymbol{D}$ is the diagonal matrix with entries being $+1$ or -1, depending on the corresponding filter being symmetric or antisymmetric. For clarity of presentation and without any loss of generality, all symmetric filters are permuted to be on top, i.e., $\boldsymbol{D} = \left[\begin{smallmatrix} \boldsymbol{I}_S & \boldsymbol{0} \\ \boldsymbol{0} & -\boldsymbol{I}_A \end{smallmatrix}\right]$, where S stands for the number of symmetric filters, and A stands for the number of antisymmetric filters. S and A have to satisfy the necessary constraints in Table I: $S = A = M/2$ if M is even; $S = (M+1)/2$ and $A = (M-1)/2$ if M is odd.

Similarly, the LP property of $\boldsymbol{E}(z)$ is equivalent to

$$\begin{aligned}
&\boldsymbol{E}(z) = z^{-(K+N-1)}\boldsymbol{D}\boldsymbol{E}\left(z^{-1}\right)\boldsymbol{J} \\
\iff\ &\boldsymbol{E}(z) = z^{-(K+N-1)}\boldsymbol{D}\boldsymbol{G}(z^{-1})\boldsymbol{F}\left(z^{-1}\right)\boldsymbol{J} \\
\iff\ &\boldsymbol{E}(z) = z^{-N}\boldsymbol{D}\boldsymbol{G}\left(z^{-1}\right)z^{-(K-1)}\boldsymbol{F}\left(z^{-1}\right)\boldsymbol{J} \\
\iff\ &\boldsymbol{E}(z) = z^{-N}\boldsymbol{D}\boldsymbol{G}\left(z^{-1}\right)\boldsymbol{D}z^{-(K-1)}\boldsymbol{D}\boldsymbol{F}\left(z^{-1}\right)\boldsymbol{J} \\
\iff\ &\boldsymbol{E}(z) = z^{-N}\boldsymbol{D}\boldsymbol{G}\left(z^{-1}\right)\boldsymbol{D}\boldsymbol{F}(z).
\end{aligned}$$

Thus, for $\boldsymbol{E}(z)$ to have LP, it is necessary and sufficient that

$$\boldsymbol{G}(z) = z^{-N}\boldsymbol{D}\boldsymbol{G}\left(z^{-1}\right)\boldsymbol{D}. \tag{6}$$

Now, substituting $\boldsymbol{G}(z) = \sum_{i=0}^{N}\boldsymbol{A}_i z^{-i}$ into the right-hand side of (6) yields

$$\begin{aligned}
\boldsymbol{G}(z) &= z^{-N}\boldsymbol{D}\left(\sum_{i=0}^{N}\boldsymbol{A}_i z^{i}\right)\boldsymbol{D} \\
&= \boldsymbol{D}\left(\sum_{i=0}^{N}\boldsymbol{A}_i z^{i-N}\right)\boldsymbol{D} \\
&= \boldsymbol{D}\left(\sum_{i=0}^{N}\boldsymbol{A}_{N-i} z^{-i}\right)\boldsymbol{D} \\
&= \sum_{i=0}^{N}(\boldsymbol{D}\boldsymbol{A}_{N-i}\boldsymbol{D})z^{-i} \\
&\Longrightarrow \boldsymbol{A}_i = \boldsymbol{D}\boldsymbol{A}_{N-i}\boldsymbol{D}.
\end{aligned} \tag{7}$$

In other words, the specific form of $\boldsymbol{G}(z)$ in (6) imposes interesting symmetric constraints on the matrices $\boldsymbol{A}_i$. □

Theorem I already presents a strong result. It states that the building block $\boldsymbol{G}(z)$ with the three aforementioned properties has a unique structure with respect to the propagation of LP and PR—there exists no other solution. In addition, note that the order N of $\boldsymbol{G}(z)$ is purposely chosen to be arbitrary so that it can cover all classes of FB that may be unfactorizable with order-1 structures. For example, according to Table I, an odd-channel even-length LPPR system does not exist. Hence, it is not possible to construct a lattice with order-1 building blocks when M is odd. The minimum length increment in this case has to be $2M$, and the simplest possible structure must have order of at least 2. Sections III and IV discuss in details more specific cases with order-1 and order-2 LP-propagating structures, respectively.

III. Lattice Structure for Even-Channel LPPRFB

Let us assume further that M is even. In this case, possible solutions must have $M/2$ symmetric and $M/2$ antisymmetric filters, as indicated in Table I. Furthermore, we know that LPPRFB exists for every integer $K \geq 1$ [4]–[6], i.e., these FB can be factored by order-1 structure. If $N = 1$ in (7), $\boldsymbol{A}_1 = \boldsymbol{D}\boldsymbol{A}_0\boldsymbol{D}$. Then, $\boldsymbol{G}(z)$ takes the general form of $\boldsymbol{G}(z) = \boldsymbol{A}_0 + z^{-1}\boldsymbol{D}\boldsymbol{A}_0\boldsymbol{D}$.

Fact: $\boldsymbol{G}(z)$ is not FIR invertible if $\boldsymbol{A}_0$ has full rank.

Suppose that $\boldsymbol{G}(z)$ is FIR invertible, and without loss of generality, let $\boldsymbol{G}^{-1}(z) = \boldsymbol{B}_0 + z\boldsymbol{D}\boldsymbol{B}_0\boldsymbol{D}$ (keep in mind that the synthesis filters have LP as well). Since $\boldsymbol{G}^{-1}(z)\boldsymbol{G}(z) = \boldsymbol{I}$, evaluating the equation with like powers of z yields

$$\begin{aligned}
\boldsymbol{B}_0\boldsymbol{A}_0 + \boldsymbol{D}\boldsymbol{B}_0\boldsymbol{A}_0\boldsymbol{D} &= \boldsymbol{I} \\
\boldsymbol{A}_0\boldsymbol{B}_0 + \boldsymbol{D}\boldsymbol{A}_0\boldsymbol{B}_0\boldsymbol{D} &= \boldsymbol{I}
\end{aligned} \tag{8}$$

and

$$\begin{aligned}
\boldsymbol{B}_0\boldsymbol{D}\boldsymbol{A}_0 &= \boldsymbol{0} \\
\boldsymbol{A}_0\boldsymbol{D}\boldsymbol{B}_0 &= \boldsymbol{0}.
\end{aligned} \tag{9}$$

If $\boldsymbol{A}_0$ is full rank, $\boldsymbol{B}_0 = \boldsymbol{0}$, and (8) becomes inconsistent. □

Moreover, according to Sylvester's rank theorem [24], we can easily prove that $\rho(\boldsymbol{A}_0) + \rho(\boldsymbol{B}_0) \leq M$ from (9). Our interest is in the most general solution, and there should be no bias on a particular bank. Hence, we propose the following solution with $\rho(\boldsymbol{A}_0) = \rho(\boldsymbol{B}_0) \leq M/2$:

$$\boldsymbol{A}_0 = \tfrac{1}{2}\begin{bmatrix} \boldsymbol{U} & \boldsymbol{U} \\ \boldsymbol{V} & \boldsymbol{V} \end{bmatrix} \tag{10}$$

where $\boldsymbol{U}$ and $\boldsymbol{V}$ are arbitrary $M/2 \times M/2$ matrices. We will later prove that the choice of $\boldsymbol{A}_0$ in (10) is indeed the most general solution (see *Lemma I* in the Appendix). Now $\boldsymbol{G}(z) = \boldsymbol{A}_0 + z^{-1}\boldsymbol{D}\boldsymbol{A}_0\boldsymbol{D}$ can be factorized as follows:

$$\begin{aligned}
\boldsymbol{G}(z) &= \tfrac{1}{2}\begin{bmatrix} \boldsymbol{U} + z^{-1}\boldsymbol{U} & \boldsymbol{U} - z^{-1}\boldsymbol{U} \\ \boldsymbol{V} - z^{-1}\boldsymbol{V} & \boldsymbol{V} + z^{-1}\boldsymbol{V} \end{bmatrix} \\
&= \tfrac{1}{2}\begin{bmatrix} \boldsymbol{U} & \boldsymbol{0} \\ \boldsymbol{0} & \boldsymbol{V} \end{bmatrix}\begin{bmatrix} \boldsymbol{I} & \boldsymbol{I} \\ \boldsymbol{I} & -\boldsymbol{I} \end{bmatrix}\begin{bmatrix} \boldsymbol{I} & \boldsymbol{0} \\ \boldsymbol{0} & z^{-1}\boldsymbol{I} \end{bmatrix}\begin{bmatrix} \boldsymbol{I} & \boldsymbol{I} \\ \boldsymbol{I} & -\boldsymbol{I} \end{bmatrix} \\
&\triangleq \tfrac{1}{2}\boldsymbol{\Phi}\boldsymbol{W}\boldsymbol{\Lambda}(z)\boldsymbol{W}.
\end{aligned} \tag{11}$$

All of the delays are now contained in $\boldsymbol{\Lambda}(z)$, whereas $\boldsymbol{W}$ resembles the famous "butterfly" matrix in the FFT implementation. Since $\boldsymbol{W}$ and $\boldsymbol{\Lambda}(z)$ are paraunitary, $\boldsymbol{G}(z)$ is invertible if and only if $\boldsymbol{\Phi}$ is invertible, i.e., $\boldsymbol{U}$ and $\boldsymbol{V}$ are invertible. A cascade of $(K-1)$ blocks $\boldsymbol{G}_i = (1/2)\boldsymbol{\Phi}_i\boldsymbol{W}\boldsymbol{\Lambda}(z)\boldsymbol{W}$ and a zero-order initial block $\boldsymbol{E}_0$ generates the polyphase matrix of an even-channel LPPRFB with filter length $L = KM$:

$$\begin{aligned}
\boldsymbol{E}(z) &= \boldsymbol{G}_{K-1}(z)\boldsymbol{G}_{K-2}(z)\cdots\boldsymbol{G}_2(z)\boldsymbol{G}_1(z)\boldsymbol{E}_0 \\
&= \prod_{i=K-1}^{1}\boldsymbol{G}_i(z)\boldsymbol{E}_0.
\end{aligned} \tag{12}$$

The starting block $\boldsymbol{E}_0$ has no delay element, represents an LPPRFB of length M, and was often chosen to be the DCT [5], [16], [17]. The most general $\boldsymbol{E}_0$ that satisfies (4) has the form

$$\begin{aligned}\boldsymbol{E}_0 &= \frac{1}{\sqrt{2}}\begin{bmatrix}\boldsymbol{U}_0 & \boldsymbol{U}_0\boldsymbol{J}\\ \boldsymbol{V}_0\boldsymbol{J} & -\boldsymbol{V}_0\end{bmatrix}\\ &= \frac{1}{\sqrt{2}}\begin{bmatrix}\boldsymbol{U}_0 & \boldsymbol{0}\\ \boldsymbol{0} & \boldsymbol{V}_0\end{bmatrix}\begin{bmatrix}\boldsymbol{I} & \boldsymbol{J}\\ \boldsymbol{J} & -\boldsymbol{I}\end{bmatrix}.\end{aligned} \tag{13}$$

For $\boldsymbol{E}_0$ to have PR, $\boldsymbol{U}_0$ and $\boldsymbol{V}_0$ again have to be invertible. The polyphase matrix of the corresponding causal synthesis bank is then

$$\begin{aligned}\boldsymbol{R}(z) &= z^{-(K-1)}\boldsymbol{E}_0^{-1}\boldsymbol{G}_1^{-1}(z)\boldsymbol{G}_2^{-1}(z)\cdots\boldsymbol{G}_{K-2}^{-1}(z)\boldsymbol{G}_{K-1}^{-1}(z)\\ &= \boldsymbol{E}_0^{-1}\prod_{i=1}^{K-1} z^{-1}\boldsymbol{G}_i^{-1}(z).\end{aligned} \tag{14}$$

The complete lattice for both analysis and synthesis bank is depicted in Fig. 4. Results in (11)–(14) should not come as a surprise. The factorization is very similar to the GenLOT's lattice structure [5] in the more restrictive case of paraunitary FB. In that case, the authors obtained PU systems by enforcing orthogonality on $\boldsymbol{\Phi}_i$. Now, we have to show that the proposed factorization does cover all possible solutions in the problem formulation of Section II by proving the converse of the result in (12).

Theorem II: The analysis polyphase matrix $\boldsymbol{E}(z)$ of any even-channel FIR LPPRFB with all analysis and synthesis filters of length $L = KM$ can always be factored as $\boldsymbol{E}(z) = \prod_{i=K-1}^{1}\boldsymbol{G}_i(z)\boldsymbol{E}_0$, where $\boldsymbol{G}_i(z)$ is as in (11), and $\boldsymbol{E}_0$ is as in (13). The corresponding synthesis polyphase matrix is $\boldsymbol{R}(z) = \boldsymbol{E}_0^{-1}\prod_{i=1}^{K-1} z^{-1}\boldsymbol{G}_i^{-1}(z)$.

The proof of Theorem II, where the LP and length constraint on the filters play a crucial role, is presented in the Appendix. We can now proceed without any loss of continuity.

Theorem III: The factorization in (12) is minimal, i.e., the resulting lattice structure employs the fewest number of delays in its implementation.

Proof: A structure is said to be minimal if the number of delays used is equal to the degree of the transfer function. For the class of systems in consideration, it can be easily proven [25] that

$$\deg(\boldsymbol{E}(z)) = \deg(|\boldsymbol{E}(z)|).$$

Using the symmetry property of the polyphase matrix in (4), we have

$$\begin{aligned}\deg(\boldsymbol{E}(z)) &= \deg(|\boldsymbol{E}(z)|)\\ &= \deg\left(z^{-(K-1)}|\boldsymbol{D}|\left|\boldsymbol{E}\left(z^{-1}\right)\right||\boldsymbol{J}|\right).\end{aligned}$$

Therefore

$$\deg(\boldsymbol{E}(z)) = M(K-1) - \deg(\boldsymbol{E}(z))$$

which leads to $\deg(\boldsymbol{E}(z)) = (M(K-1))/2$. In our factorization, there are $(K-1)$ building blocks $\boldsymbol{G}_i(z)$, where each employs $M/2$ delays. Thus, the total number of delays in use is $(M(K-1))/2$, leading to the conclusion that the factorization is minimal. □

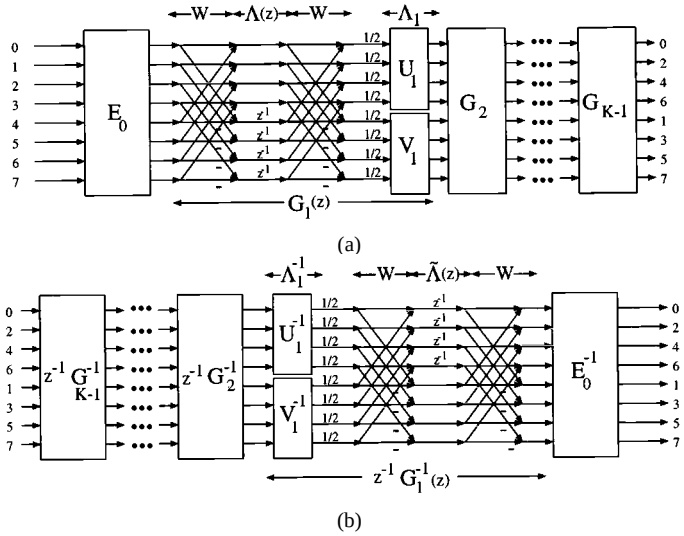

Fig. 4. General lattice structure for even-channel LPPRFB. (a) Analysis bank. (b) Synthesis bank.

IV. Lattice Structure for Odd-Channel LPPRFB

Suppose M is now odd. As previously mentioned in Section II, the minimum order of the propagating structure $\boldsymbol{G}(z)$ is 2, i.e., $\boldsymbol{G}(z) = \boldsymbol{A}_0 + \boldsymbol{A}_1 z^{-1} + \boldsymbol{A}_2 z^{-2}$. According to Theorem I, the following relationships must hold:

$$\boldsymbol{A}_2 = \boldsymbol{D}\boldsymbol{A}_0\boldsymbol{D} \tag{15}$$

$$\boldsymbol{A}_1 = \boldsymbol{D}\boldsymbol{A}_1\boldsymbol{D} \tag{16}$$

where we are is reminded that

$$\boldsymbol{D} = \begin{bmatrix}\boldsymbol{I}_{(M+1)/2} & \boldsymbol{0}\\ \boldsymbol{0} & -\boldsymbol{I}_{(M-1)/2}\end{bmatrix}.$$

We expect the factorization to be quite similar to the even-channel case's. The main difference is that the system now has one more symmetric filter. Therefore, consider the factorization in

$$\begin{aligned}\boldsymbol{G}(z) = \tfrac{1}{2}&\begin{bmatrix}\boldsymbol{U} & \boldsymbol{u}_1 & \boldsymbol{0}\\ \boldsymbol{u}_2 & u_0 & \boldsymbol{0}\\ \boldsymbol{0} & \boldsymbol{0} & \boldsymbol{V}\end{bmatrix}\begin{bmatrix}\boldsymbol{I}+z^{-1}\boldsymbol{I} & \boldsymbol{0} & \boldsymbol{I}-z^{-1}\boldsymbol{I}\\ \boldsymbol{0} & 2 & \boldsymbol{0}\\ \boldsymbol{I}-z^{-1}\boldsymbol{I} & \boldsymbol{0} & \boldsymbol{I}+z^{-1}\boldsymbol{I}\end{bmatrix}\\ \times\tfrac{1}{2}&\begin{bmatrix}\boldsymbol{Q} & \boldsymbol{q}_1 & \boldsymbol{0}\\ \boldsymbol{q}_2 & q_0 & \boldsymbol{0}\\ \boldsymbol{0} & \boldsymbol{0} & \boldsymbol{R}\end{bmatrix}\begin{bmatrix}\boldsymbol{I}+z^{-1}\boldsymbol{I} & \boldsymbol{0} & \boldsymbol{I}-z^{-1}\boldsymbol{I}\\ \boldsymbol{0} & 2z^{-1} & \boldsymbol{0}\\ \boldsymbol{I}-z^{-1}\boldsymbol{I} & \boldsymbol{0} & \boldsymbol{I}+z^{-1}\boldsymbol{I}\end{bmatrix}\end{aligned} \tag{17}$$

where matrices $\boldsymbol{U}$, $\boldsymbol{V}$, $\boldsymbol{Q}$, $\boldsymbol{R}$, and $\boldsymbol{I}$ have size $((M-1)/2)\times((M-1)/2)$; $\boldsymbol{u}_1$ and $\boldsymbol{q}_1$ are of size $((M-1)/2)\times 1$; $\boldsymbol{u}_2$ and $\boldsymbol{q}_2$ are of size $1\times((M-1)/2)$; u_0 and q_0 are scalars.

This particular choice of $\boldsymbol{G}(z)$ results in (18)–(20), shown at the bottom of the page. For (15) and (16) to hold simultaneously, the general solution is to set both $\boldsymbol{q}_1$ and $\boldsymbol{q}_2$ to $\boldsymbol{0}$. (Another solution is to choose $\boldsymbol{q}_1$, $\boldsymbol{u}_1$, and u_0 to be $\boldsymbol{0}$. However, annihilating $\boldsymbol{u}_1$ and u_0 also automatically eliminates $\boldsymbol{q}_2$ from the set of free

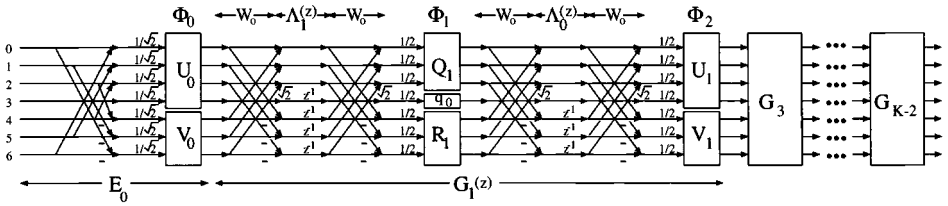

Fig. 5. Lattice structure for odd-channel LPPRFB.

parameters.) With $\boldsymbol{q}_1 = \boldsymbol{q}_2^T = \boldsymbol{0}$, the simplified factorization takes the form

$$\boldsymbol{G}(z) = \tfrac{1}{4}\begin{bmatrix} \boldsymbol{U} & \boldsymbol{u}_1 & \boldsymbol{0} \\ \boldsymbol{u}_2 & u_0 & \boldsymbol{0} \\ \boldsymbol{0} & \boldsymbol{0} & \boldsymbol{V} \end{bmatrix} \begin{bmatrix} \boldsymbol{I}+z^{-1}\boldsymbol{I} & \boldsymbol{0} & \boldsymbol{I}-z^{-1}\boldsymbol{I} \\ \boldsymbol{0} & 2 & \boldsymbol{0} \\ \boldsymbol{I}-z^{-1}\boldsymbol{I} & \boldsymbol{0} & \boldsymbol{I}+z^{-1}\boldsymbol{I} \end{bmatrix} \times \begin{bmatrix} \boldsymbol{Q} & \boldsymbol{0} & \boldsymbol{0} \\ \boldsymbol{0} & q_0 & \boldsymbol{0} \\ \boldsymbol{0} & \boldsymbol{0} & \boldsymbol{R} \end{bmatrix} \begin{bmatrix} \boldsymbol{I}+z^{-1}\boldsymbol{I} & \boldsymbol{0} & \boldsymbol{I}-z^{-1}\boldsymbol{I} \\ \boldsymbol{0} & 2z^{-1} & \boldsymbol{0} \\ \boldsymbol{I}-z^{-1}\boldsymbol{I} & \boldsymbol{0} & \boldsymbol{I}+z^{-1}\boldsymbol{I} \end{bmatrix}. \tag{21}$$

The two matrices containing delay elements z^{-1} can be factored further as

$$\begin{aligned} &\begin{bmatrix} \boldsymbol{I}+z^{-1}\boldsymbol{I} & \boldsymbol{0} & \boldsymbol{I}-z^{-1}\boldsymbol{I} \\ \boldsymbol{0} & 2 & \boldsymbol{0} \\ \boldsymbol{I}-z^{-1}\boldsymbol{I} & \boldsymbol{0} & \boldsymbol{I}+z^{-1}\boldsymbol{I} \end{bmatrix} \\ &\quad = \begin{bmatrix} \boldsymbol{I} & \boldsymbol{0} & \boldsymbol{I} \\ \boldsymbol{0} & \sqrt{2} & \boldsymbol{0} \\ \boldsymbol{I} & \boldsymbol{0} & -\boldsymbol{I} \end{bmatrix} \begin{bmatrix} \boldsymbol{I} & \boldsymbol{0} & \boldsymbol{0} \\ \boldsymbol{0} & 1 & \boldsymbol{0} \\ \boldsymbol{0} & \boldsymbol{0} & z^{-1}\boldsymbol{I} \end{bmatrix} \begin{bmatrix} \boldsymbol{I} & \boldsymbol{0} & \boldsymbol{I} \\ \boldsymbol{0} & \sqrt{2} & \boldsymbol{0} \\ \boldsymbol{I} & \boldsymbol{0} & -\boldsymbol{I} \end{bmatrix} \\ &\quad \triangleq \boldsymbol{W}_o \boldsymbol{\Lambda}_0(z) \boldsymbol{W}_o \end{aligned} \tag{22}$$

and

$$\begin{aligned} &\begin{bmatrix} \boldsymbol{I}+z^{-1}\boldsymbol{I} & \boldsymbol{0} & \boldsymbol{I}-z^{-1}\boldsymbol{I} \\ \boldsymbol{0} & 2z^{-1} & \boldsymbol{0} \\ \boldsymbol{I}-z^{-1}\boldsymbol{I} & \boldsymbol{0} & \boldsymbol{I}+z^{-1}\boldsymbol{I} \end{bmatrix} \\ &\quad = \begin{bmatrix} \boldsymbol{I} & \boldsymbol{0} & \boldsymbol{I} \\ \boldsymbol{0} & \sqrt{2} & \boldsymbol{0} \\ \boldsymbol{I} & \boldsymbol{0} & -\boldsymbol{I} \end{bmatrix} \begin{bmatrix} \boldsymbol{I} & \boldsymbol{0} & \boldsymbol{0} \\ \boldsymbol{0} & z^{-1} & \boldsymbol{0} \\ \boldsymbol{0} & \boldsymbol{0} & z^{-1}\boldsymbol{I} \end{bmatrix} \begin{bmatrix} \boldsymbol{I} & \boldsymbol{0} & \boldsymbol{I} \\ \boldsymbol{0} & \sqrt{2} & \boldsymbol{0} \\ \boldsymbol{I} & \boldsymbol{0} & -\boldsymbol{I} \end{bmatrix} \\ &\quad \triangleq \boldsymbol{W}_o \boldsymbol{\Lambda}_1(z) \boldsymbol{W}_o. \end{aligned} \tag{23}$$

In both (22) and (23), all factors have trivial orthogonal inverses. Hence, further enforcement of the PR property on $\boldsymbol{G}(z)$ requires $\left[\begin{smallmatrix} \boldsymbol{U} & \boldsymbol{u}_1 \\ \boldsymbol{u}_2 & u_0 \end{smallmatrix}\right]$, $\boldsymbol{V}$, $\boldsymbol{Q}$, and $\boldsymbol{R}$ to be invertible, whereas q_0 is a nonzero scalar. Higher order systems can be constructed by cascading more $\boldsymbol{G}(z)$ stages:

$$\boldsymbol{E}(z) = \boldsymbol{G}_{K-2}(z)\boldsymbol{G}_{K-4}(z) \cdots \boldsymbol{G}_3(z)\boldsymbol{G}_1(z)\boldsymbol{E}_0, \qquad K \text{ odd} \tag{24}$$

and the corresponding synthesis polyphase matrix is given by

$$\boldsymbol{R}(z) = z^{-(K-1)}\boldsymbol{E}_0^{-1}\boldsymbol{G}_1^{-1}(z)\boldsymbol{G}_3^{-1}(z) \cdots \boldsymbol{G}_{K-4}^{-1}(z)\boldsymbol{G}_{K-2}^{-1}(z). \tag{25}$$

Again, the starting block $\boldsymbol{E}_0$ of the cascade does not contain any delay; it represents the simplest LPPRFB with all filters of length M. The general solution for $\boldsymbol{E}_0$ is

$$\begin{aligned} \boldsymbol{E}_0 &= \begin{bmatrix} \boldsymbol{U}_0 & \boldsymbol{u}_{01}\sqrt{2} & \boldsymbol{U}_0\boldsymbol{J} \\ \boldsymbol{u}_{02} & u_{00}\sqrt{2} & \boldsymbol{u}_{02}\boldsymbol{J} \\ -\boldsymbol{V}_0\boldsymbol{J} & \boldsymbol{0} & \boldsymbol{V}_0 \end{bmatrix} \\ &= \frac{1}{\sqrt{2}} \begin{bmatrix} \boldsymbol{U}_0 & \boldsymbol{u}_{01} & \boldsymbol{0} \\ \boldsymbol{u}_{02} & u_{00} & \boldsymbol{0} \\ \boldsymbol{0} & \boldsymbol{0} & \boldsymbol{V}_0 \end{bmatrix} \begin{bmatrix} \boldsymbol{I} & \boldsymbol{0} & \boldsymbol{J} \\ \boldsymbol{0} & \sqrt{2} & \boldsymbol{0} \\ -\boldsymbol{J} & \boldsymbol{0} & \boldsymbol{I} \end{bmatrix} \end{aligned} \tag{26}$$

where $\left[\begin{smallmatrix} \boldsymbol{U}_0 & \boldsymbol{u}_{01} \\ \boldsymbol{u}_{02} & u_{00} \end{smallmatrix}\right]$ and $\boldsymbol{V}_0$ need to be invertible. For fast-computable transform, $\boldsymbol{E}_0$ can be chosen as the $M \times M$ DCT coefficient matrix.

The full lattice structure for the analysis bank is depicted in Fig. 5. The synthesis bank can be obtained by reversing the signal flow. In contrast to the even-channel case, the odd-channel lattice in Fig. 5 is not complete; it is still minimal, however.

Theorem IV: The factorization in (24) is minimal in terms of the number of delay elements used in the FB's implementation.

$$\boldsymbol{A}_0 = \tfrac{1}{4}\begin{bmatrix} \boldsymbol{UQ}+2\boldsymbol{u}_1\boldsymbol{q}_2+\boldsymbol{UR} & \boldsymbol{0} & \boldsymbol{UQ}+2\boldsymbol{u}_1\boldsymbol{q}_2+\boldsymbol{UR} \\ \boldsymbol{u}_2\boldsymbol{Q}+2u_0\boldsymbol{q}_2+\boldsymbol{u}_2\boldsymbol{R} & 0 & \boldsymbol{u}_2\boldsymbol{Q}+2u_0\boldsymbol{q}_2+\boldsymbol{u}_2\boldsymbol{R} \\ \boldsymbol{VQ}+\boldsymbol{VR} & \boldsymbol{0} & \boldsymbol{VQ}+\boldsymbol{VR} \end{bmatrix} \tag{18}$$

$$\boldsymbol{A}_1 = \tfrac{1}{4}\begin{bmatrix} 2\boldsymbol{UQ}+2\boldsymbol{u}_1\boldsymbol{q}_2-2\boldsymbol{UR} & 2\boldsymbol{U}\boldsymbol{q}_1+4\boldsymbol{u}_1q_0 & -2\boldsymbol{u}_1\boldsymbol{q}_2 \\ 2\boldsymbol{u}_2\boldsymbol{Q}+2u_0\boldsymbol{q}_2-2\boldsymbol{u}_2\boldsymbol{R} & 2\boldsymbol{u}_2\boldsymbol{q}_1+4u_0q_0 & -2u_0\boldsymbol{q}_2 \\ \boldsymbol{0} & 2\boldsymbol{V}\boldsymbol{q}_1 & 2\boldsymbol{VR}-2\boldsymbol{VQ} \end{bmatrix} \tag{19}$$

$$\boldsymbol{A}_2 = \tfrac{1}{4}\begin{bmatrix} \boldsymbol{UQ}+\boldsymbol{UR} & 2\boldsymbol{U}\boldsymbol{q}_1 & -\boldsymbol{UQ}-\boldsymbol{UR} \\ \boldsymbol{u}_2\boldsymbol{Q}+\boldsymbol{u}_2\boldsymbol{R} & 2\boldsymbol{u}_2\boldsymbol{q}_1 & -\boldsymbol{u}_2\boldsymbol{Q}-\boldsymbol{u}_2\boldsymbol{R} \\ -\boldsymbol{VQ}-\boldsymbol{VR} & -2\boldsymbol{V}\boldsymbol{q}_1 & \boldsymbol{VQ}+\boldsymbol{VR} \end{bmatrix} \tag{20}$$

Proof: This result comes straight from the proof of Theorem III. The degree of $\boldsymbol{E}(z)$ is $(M(K-1))/2$ for both odd and even M. In our odd-channel solution, K is always odd; there are $(K-1)/2$ "double" building blocks $\boldsymbol{G}_i(z)$, where each employs M delays [$\boldsymbol{\Lambda}_0(z)$ has $(M-1)/2$, whereas $\boldsymbol{\Lambda}_1(z)$ has $(M+1)/2$ delays]. Therefore, the total number of delays employed in the implementation is $(M(K-1))/2$. □

There are a couple of interesting side notes on the lattice in Fig. 5. First, to construct odd-channel LPPUFB (odd-channel GenLOT), we simply have to choose all free-parameter matrices $\begin{bmatrix} \boldsymbol{U}_i & \boldsymbol{u}_{i1} \\ \boldsymbol{u}_{i2} & u_{i0} \end{bmatrix}$, $\boldsymbol{V}_i$, $\boldsymbol{Q}_i$, $\boldsymbol{R}_i$, and q_i in the propagating stages $\boldsymbol{G}_i(z)$ and the starting block $\boldsymbol{E}_0$ to be orthogonal. This choice turns out to be an alternate, but equivalent, form of the factorization presented earlier in [26]. Second, the curious will immediately ponder the following: What happens at the middle of the "double" structure? Let us consider the simplest case where only half of stage $\boldsymbol{G}(z)$ is involved, i.e.,

$$\boldsymbol{E}(z) = \begin{bmatrix} \boldsymbol{Q} & \boldsymbol{0} & \boldsymbol{0} \\ \boldsymbol{0} & q_0 & \boldsymbol{0} \\ \boldsymbol{0} & \boldsymbol{0} & \boldsymbol{R} \end{bmatrix} \begin{bmatrix} \boldsymbol{I}+z^{-1}\boldsymbol{I} & \boldsymbol{0} & \boldsymbol{I}-z^{-1}\boldsymbol{I} \\ \boldsymbol{0} & 2z^{-1} & \boldsymbol{0} \\ \boldsymbol{I}-z^{-1}\boldsymbol{I} & \boldsymbol{0} & \boldsymbol{I}+z^{-1}\boldsymbol{I} \end{bmatrix} \cdot \begin{bmatrix} \boldsymbol{U}_0 & \boldsymbol{u}_{01}\sqrt{2} & \boldsymbol{U}_0\boldsymbol{J} \\ \boldsymbol{u}_{02} & u_{00}\sqrt{2} & \boldsymbol{u}_{02}\boldsymbol{J} \\ -\boldsymbol{V}_0\boldsymbol{J} & \boldsymbol{0} & \boldsymbol{V}_0 \end{bmatrix}. \tag{27}$$

The FB's corresponding coefficient matrix (transposed) is then as in (27a), shown at the bottom of the page. Interestingly, the FB still has PR because every factor in (27) is invertible. Furthermore, all filters still have LP as $\boldsymbol{P}^T$ indicates. The only trouble comes from the symmetric filter in the middle, which turns out to have only M taps. This type of system with filters of unequal lengths is outside the class of FB in consideration and is beyond the scope of this paper.

V. Parameterization of Invertible Matrices

Up until this point, we are still evasive on how to parameterize invertible matrices. In the paraunitary case, each of the $N \times N$ orthogonal matrices $\boldsymbol{U}_i$, $\boldsymbol{V}_i$ containing the free parameters is completely characterized by $(N(N-1))/2$ Givens rotations [5], as shown in Fig. 6 (drawn for $N = 4$). The parameterization of the FB into rotation angles (which are called lattice coefficients) structurally enforces the LP and PR properties, i.e., in the lattice representation, both LP and PR properties are retained regardless of coefficient quantization. From a design perspective, the lattice structure is a powerful FB design tool since the lattice coefficients can be varied independently and arbitrarily without affecting the most desirable FB characteristics. Unconstrained optimization can be applied to obtain secondary features such as high coding gain and low stopband attenuation. From a practical perspective, the lattice provides a fast, efficient, modular, and robust structure suitable for hardware implementation.

The difficulty in the biorthogonal case is obvious: How do we completely characterize a nonsingular square matrix $\boldsymbol{U}_i$ of size N? One naive solution is to choose $\boldsymbol{U}_i$'s elements as the lattice coefficients. However, there are many problems with this solution. First of all, it is difficult to guarantee exact reconstruction when the matrix elements are quantized. Second, this "parameterization" method does not provide a fast and efficient FB implementation. Furthermore, in order to obtain a high-performance FB, we have to synthesize the lattice by an optimization process to find the set of locally optimal lattice coefficients. This process typically involves thousands of iterative steps; therfore, we have to face the costly matrix inversion problem. Finally, how can we prevent the optimization process from encountering singular or near-singular matrices?

To solve the aforementioned problems, we propose a parameterization method of invertible matrices by their singular value decompositions (SVD's). Recall that every invertible matrix has an SVD representation $\boldsymbol{U}_i = \boldsymbol{U}_{i0}\boldsymbol{\Gamma}_i\boldsymbol{U}_{i1}$, where $\boldsymbol{U}_{i0}$ and $\boldsymbol{U}_{i1}$ are orthogonal matrices, and $\boldsymbol{\Gamma}_i$ is a diagonal matrix with positive elements [27]. Thus, $\boldsymbol{U}_i$ of size N can be completely characterized by $N(N-1)$ rotation angles θ_i (from $\boldsymbol{U}_{i0}$, $\boldsymbol{U}_{i1}$) and $N/2$ diagonal multipliers α_i (from $\boldsymbol{\Gamma}_i$), as illustrated in Fig. 7. Invertibility is guaranteed structurally under a mild condition—as long as none of the diagonal lattice coefficients α_i representing $\boldsymbol{\Gamma}_i$ is quantized to zero. Moreover, inverting $\boldsymbol{U}_i$ is now very fast, and singularity can be prevented by a simple cost function in the optimization process, where a penalty is assigned whenever a diagonal coefficient (or its inverse) ventures too close to zero.

In the even-channel case, under the SVD parameterization, $\boldsymbol{\Phi}_i$ can be further factorized as

$$\boldsymbol{\Phi}_i = \begin{bmatrix} \boldsymbol{U}_{i0} & \boldsymbol{0} \\ \boldsymbol{0} & \boldsymbol{V}_{i0} \end{bmatrix} \begin{bmatrix} \boldsymbol{\Gamma}_i & \boldsymbol{0} \\ \boldsymbol{0} & \boldsymbol{\Delta}_i \end{bmatrix} \begin{bmatrix} \boldsymbol{U}_{i1} & \boldsymbol{0} \\ \boldsymbol{0} & \boldsymbol{V}_{i1} \end{bmatrix}. \tag{28}$$

Again, the $M/2 \times M/2$ orthogonal matrices $\boldsymbol{U}_{i0}$, $\boldsymbol{U}_{i1}$, $\boldsymbol{V}_{i0}$, and $\boldsymbol{V}_{i1}$ are parameterized by $(M(M-2))/8$ rotations each. The diagonal matrices $\boldsymbol{\Gamma}_i$ and $\boldsymbol{\Delta}_i$ are characterized by $M/2$ positive parameters each. The detailed even-channel lattice structure is shown in Fig. 8 (drawn for $M = 8$). Each of the K cascading blocks in the lattice (including $\boldsymbol{E}_0$) has $M^2/2$ degrees of freedom. Thus, the most general M-channel LPPRFB with filter length $L = KM$ (i.e., $M \times L$ GLBT) can be parameterized by $KM^2/2 = LM/2$ parameters, as expected from the most general LP systems. The classical tradeoff between the FB's complexity and performance can be elegantly carried out by setting some of the diagonal multipliers to 1 or some of the rotation angles to 0.

$$\boldsymbol{P}^T = \begin{bmatrix} \boldsymbol{Q}\boldsymbol{U}_0 - \boldsymbol{Q}\boldsymbol{V}_0\boldsymbol{J} & \boldsymbol{Q}\boldsymbol{u}_{01} & \boldsymbol{Q}\boldsymbol{U}_0\boldsymbol{J} + \boldsymbol{Q}\boldsymbol{V}_0 & \boldsymbol{Q}\boldsymbol{U}_0 + \boldsymbol{Q}\boldsymbol{V}_0\boldsymbol{J} & \boldsymbol{Q}\boldsymbol{u}_{01} & \boldsymbol{Q}\boldsymbol{U}_0\boldsymbol{J} - \boldsymbol{Q}\boldsymbol{V}_0 \\ \boldsymbol{0} & \boldsymbol{0} & \boldsymbol{0} & q_0\boldsymbol{u}_{02} & q_0u_0 & q_0\boldsymbol{u}_{02}\boldsymbol{J} \\ \boldsymbol{R}\boldsymbol{U}_0 - \boldsymbol{R}\boldsymbol{V}_0\boldsymbol{J} & \boldsymbol{R}\boldsymbol{u}_{01} & \boldsymbol{R}\boldsymbol{U}_0\boldsymbol{J} + \boldsymbol{R}\boldsymbol{V}_0 & -\boldsymbol{R}\boldsymbol{U}_0 - \boldsymbol{R}\boldsymbol{V}_0\boldsymbol{J} & -\boldsymbol{R}\boldsymbol{u}_{01} & -\boldsymbol{R}\boldsymbol{U}_0\boldsymbol{J} + \boldsymbol{R}\boldsymbol{V}_0 \end{bmatrix} \tag{27a}$$

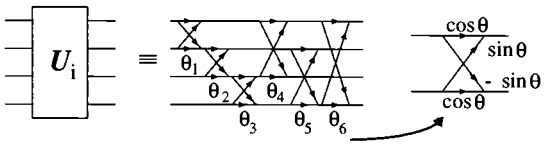

Fig. 6. Parameterization of orthogonal matrix.

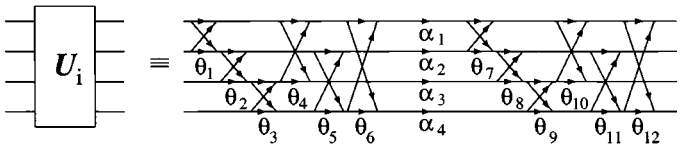

Fig. 7. Parameterization of invertible matrix.

It is also very easy to verify that all previously reported even-channel LPPRFB's rotation-based lattice structures are special cases of the new lattice. For examples, the GLT design example in [16] has $M = 8$, $K = 2$, $\boldsymbol{U}_{00}$, and $\boldsymbol{V}_{00}$ from the DCT; $\boldsymbol{U}_{01} = \boldsymbol{V}_{01} = \boldsymbol{\Gamma}_0 = \boldsymbol{\Delta}_0 = \boldsymbol{I}$; $\boldsymbol{U}_1$ and $\boldsymbol{V}_1$ parameterized as a cascade of block diagonal matrices. The LBT in [18] has $M = 8$, $K = 2$, $\boldsymbol{U}_{00}$, and $\boldsymbol{V}_{00}$ from the DCT, $\boldsymbol{U}_{01} = \boldsymbol{V}_{01} = \boldsymbol{\Gamma}_0 = \boldsymbol{I}$, $\boldsymbol{\Delta}_0 = \text{diag}[\sqrt{2} \quad 1 \quad 1 \quad 1]$, and $\boldsymbol{U}_1$, $\boldsymbol{V}_1$ orthogonal. When orthogonality is imposed, we get back GenLOT [5]. When $M = 2,$, the lattice turns into a modular form of the Type-A system lattice [8]. Comparing the novel GLBT with the biorthogonal lapped transform (BOLT) in [28] reveals several fundamental differences.

i) The GLBT's analysis polyphase matrix is not restricted to have order 2.
ii) The GLBT have LP analysis and synthesis filters of the same length.
iii) The factorization approaches are totally dissimilar.

The odd-channel case is more complicated. An order-2 stage $\boldsymbol{G}_i(z)$ contains $((M+1)/2)^2 + 3((M-1)/2)^2 + 1 = (M^2 - M + 2)$ free parameters, whereas $\boldsymbol{E}_0$ has $((M+1)/2)^2 + ((M-1)/2)^2 = (M^2+1)/2$. Since there are $(M+1)/2$ symmetric filters, $(M-1)/2$ antisymmetric filters, and all of them have LP, the most general solution is expected to have $((M+1)/2)((KM+1)/2) + ((M-1)/2)((KM-1)/2) = (KM^2+1)/2$ free parameters. Subtracting $(M^2+1)/2$ parameters that belong to the initial stage $\boldsymbol{E}_0$, each stage $\boldsymbol{G}_i(z)$ [there are $(K-1)/2$ of them] should possess M^2 degrees of freedom. Hence, each stage in our proposed solution in the previous section is off by $(M-2)$ parameters.

VI. Design and Application in Image Coding

A. FB Optimization

Any realization of the lattice coefficient set $\{\theta_i, \alpha_i\}$ in the previous two sections results in an LPPR system. However, for the FB to have high practical value, several other properties are also needed. High-performance FB can be obtained using unconstrained nonlinear optimization, where the lattice coefficients are the free parameters. Since image compression is the main concern in this paper, the cost function is a weighted linear combination of coding gain, DC leakage, attenuation around mirror frequencies, and stopband attenuation, all of which are well-known desired properties in yielding the best reconstructed image quality [2], [29]

$$C_{\text{overall}} = \alpha_1 C_{\text{coding gain}} + \alpha_2 C_{\text{DC}} + \alpha_3 C_{\text{mirror}} + \alpha_4 C_{\text{analysis stopband}} + \alpha_5 C_{\text{synthesis stopband}}. \tag{29}$$

Among these criteria, higher coding gain correlates most consistently with higher objective performance (PSNR). Transforms with higher coding gain compact more energy into a fewer number of coefficients, and the more significant bits of those coefficients always get transmitted first in the progressive transmission framework employed in the later section. All design examples in this paper are obtained with a version of the generalized coding gain formula in [30]

$$C_{\text{coding gain}} = 10 \log_{10} \frac{\sigma_x^2}{\left(\prod_{k=0}^{M-1} \sigma_{x_i}^2 \|f_i\|^2 \right)^{1/M}} \tag{30}$$

where

σ_x^2 variance of the input signal;
$\sigma_{x_i}^2$ variance of the ith subband;
$\|f_i\|^2$ norm of the ith synthesis filter.

The signal $x[n]$ is the commonly-used AR(1) process with intersample autocorrelation coefficient $\rho = 0.95$ [19].

Low DC leakage and high attenuation near the mirror frequencies are not as essential to the coder's objective performance as coding gain. However, they do improve the visual quality of the reconstructed image significantly by eliminating annoying blocking and checkerboard artifacts. Finally, the stopband attenuation cost helps in improving the signal decorrelation, decreasing the amount of aliasing, and enhancing the smoothness of the filters. These cost functions are defined as

$$C_{\text{DC}} = \sum_{i=1}^{M-1} \sum_{n=0}^{L-1} h_i[n] \tag{31}$$

$$C_{\text{mirror}} = \sum_{i=0}^{M-1} |H_i(e^{j\omega_m})|^2, \qquad \omega_m = \frac{2\pi m}{M} \quad 1 \le m \le \frac{M}{2} \tag{32}$$

$$C_{\text{analysis stopband}} = \sum_{i=0}^{M-1} \int_{\omega \in \Omega_{\text{stopband}}} W_i^a(e^{j\omega}) \cdot |H_i(e^{j\omega})|^2 \, d\omega \tag{33}$$

$$C_{\text{synthesis stopband}} = \sum_{i=0}^{M-1} \int_{\omega \in \Omega_{\text{stopband}}} W_i^s(e^{j\omega}) \cdot |F_i(e^{j\omega})|^2 \, d\omega. \tag{34}$$

The two simple functions $W_i^a(e^{j\omega})$ and $W_i^s(e^{j\omega})$ are used to enforce the weighting of the stopband attenuation of the analysis and synthesis bank, respectively.

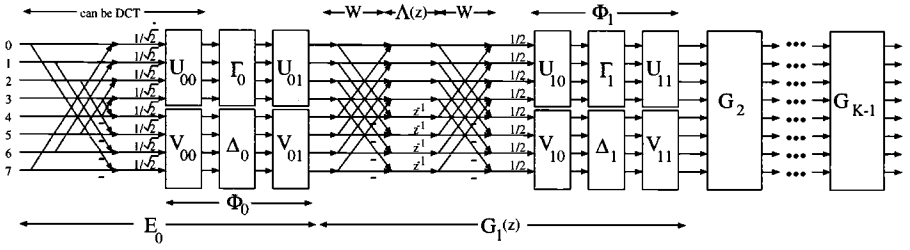

Fig. 8. Detailed lattice structure for even-channel LPPRFB.

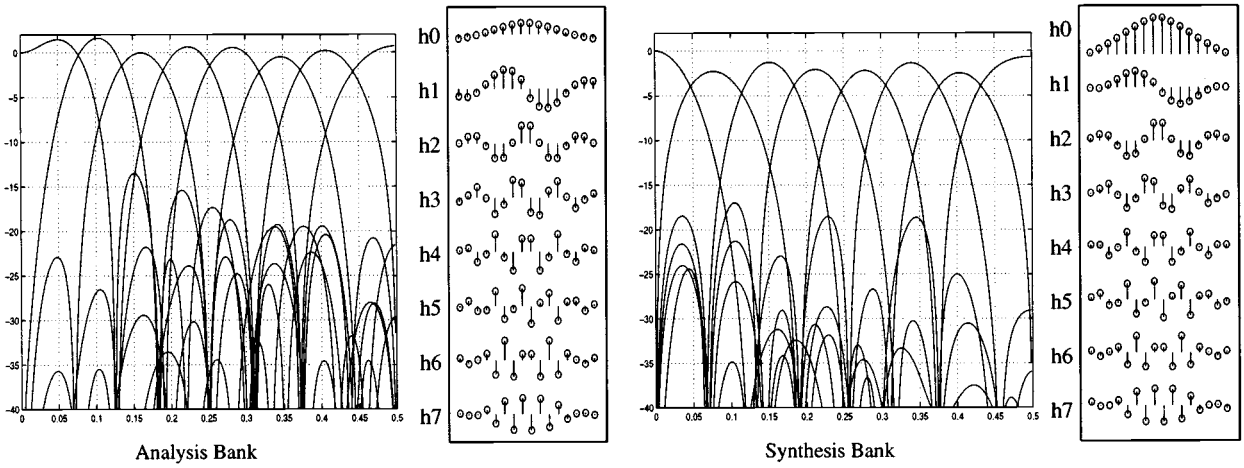

Fig. 9. Design example I: $M = 8$ $L = 16$ optimized for coding gain, DC attenuation, mirror frequency attenuation, and stopband attenuation.

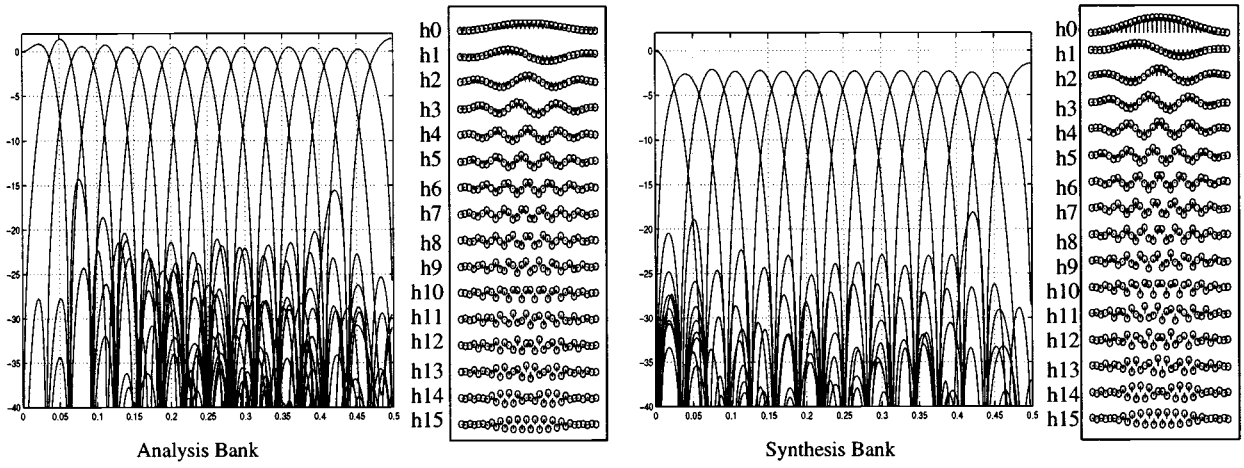

Fig. 10. Design example II: $M = 16$ $L = 32$ optimized for coding gain, DC and mirror frequency attenuation, and stopband attenuation.

B. Design Examples

Figs. 9–14 present several design examples obtained from nonlinear optimization of the new lattice coefficients with various cost functions. Fig. 9 shows design example I: an 8-channel LPPRFB with 16-tap filters (8 × 16 GLBT). Fig. 10 shows design example II with 16 channels and filter length 32 (16 × 32 GLBT). Both FB's are DCT-based and are obtained from a combinatorial cost function where the coding gain is given highest priority. The two design examples illustrate the tremendous degree of flexibility that the new biorthogonal class of LT enjoys over its orthogonal relative in previous works [4]–[6]. The analysis bank is designed to maximize coding gain, minimize the DC leakage, and maximize the stopband attenuation in low frequency bands where there is usually a high concentration of image energy. On the other hand, the synthesis bank is designed to have its filters decaying asymptotically to zero to completely eliminate blocking artifacts. Furthermore, the stopband attenuation in high-frequency synthesis bands is also maximized so that the resulting synthesis filters are generally smooth, leading to more visually pleasant reconstructed images. The 8 × 16 GLBT in design example I, if optimized for pure coding gain, can attain 9.63 dB , which equals the coding gain reported on optimal biorthogonal systems in [31]. However, the 8 × 16 LBT in [31] was obtained by a direct constrained optimization on the filter coefficients; therefore, it might only be near-PR, and it certainly

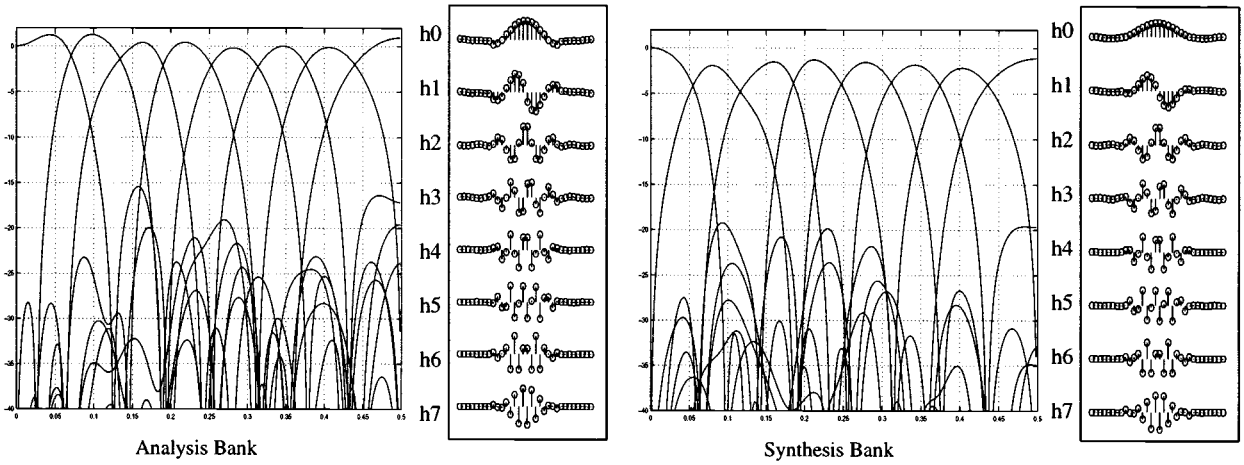

Fig. 11. Design example III: $M = 8$ $L = 32$ optimized for coding gain, DC attenuation, mirror frequency attenuation, and stopband attenuation.

TABLE II
COMPARISON OF VARIOUS TRANSFORM PROPERTIES

Transform Properties	Transforms							
	8x8 DCT	8x16 LOT	8x40 GenLOT	8x16 GLBT (I)	16x32 GLBT (II)	8x32 GLBT (III)	8x32 GLBT (IV)	7x21 GLBT (V)
Coding Gain (dB)	8.83	9.22	9.52	9.62	9.96	9.63	9.33	9.50
DC Attenuation (-dB)	310.62	312.56	322.10	327.40	303.32	327.57	35.92	37.94
Stopband Attenuation (-dB)	9.96	19.38	16.18	13.50	14.28	15.43	31.27	11.97
Mirror Freq. Attenuation (-dB)	322.10	317.24	317.24	55.54	302.35	43.84	23.83	16.45

does not have a fast, efficient, and robust implementation. In design example I, 0.01 dB of coding gain has been sacrificed for high attenuation at DC, near DC, and mirror frequencies to ensure a high level of perceptual performance in image coding. In the 16 × 32 case, our GLBT in Fig. 10 achieves an impressive coding gain of 9.96 dB.

GLBT design examples with longer filter length are shown in Figs. 11 and 12. While increasing the GLBT length only improves the coding gain marginally (see design example III in Fig. 11), it helps tremendously in the case of stopband attenuation (where longer filters are always beneficial), as attested to by design example IV in Fig. 12.

Two odd-channel FB are presented in Figs. 13 and 14. Design example V in Fig. 13 is a seven-channel 21-tap LPPRFB optimized for maximum coding gain and high stopband attenuation near DC for the analysis bank and near π for the synthesis bank. Hence, the synthesis basis functions are much smoother than the analysis. Design example VI in Fig. 14 has five channels and filters of 15 taps optimized for coding gain and DC attenuation. Various properties of high-performance design examples are compiled in Table II; the DCT [20], the LOT [19], and the 8 × 40 GenLOT [33] are included for comparison purposes.

C. Application in Image Coding

To test the performance of the new family of LT's, new GLBT's are incorporated into the block-transform progressive coding framework described in [32] and [33], where each block of lapped transform coefficients is treated analogously to a tree of wavelet coefficients. The resulting GLBT-based embedded coders provide unrivaled objective and subjective performance, as indicated in Table III and Fig. 15. For a smooth image like Lena, which the wavelet transform can sufficiently decorrelate, the best wavelet-based embedded coder SPIHT [21] provides a comparable performance. However, for a highly textured image like Barbara, the 16 × 32 GLBT coder can provide a PSNR gain of around 2.5 dB over a wide range of bit rates. The visual reconstructed image quality is also superior: texture is beautifully preserved, blocking is completely eliminated, and ringing is barely noticeable. Compared with the optimal 8 × 40 GenLOT in [33], the 8 × 16 GLBT in Fig. 9 already offers a comparable performance at a much lower level of computational complexity. Compared with the dyadic wavelets in the SPIHT coder, the GLBT can be viewed as a transform replacement for higher performance and comparable complexity. Higher performance with nondyadic (full-tree) association of filter banks is possible, but such a system incur a high computational burden. In this light, the GLBT proves itself as a compact and efficient M-band invertible transformation in image compression. More objective and subjective evaluation of GLBT-based progressive coders can be found at http://thanglong.ece.jhu.edu/Coder/.

VII. CONCLUSIONS

This paper presents general lattice structures for M-channel LPPRFB's with all analysis and synthesis filters of the same length $L = KM$. The novel lattice based on the SVD provides a fast, robust, efficient, and modular implementation

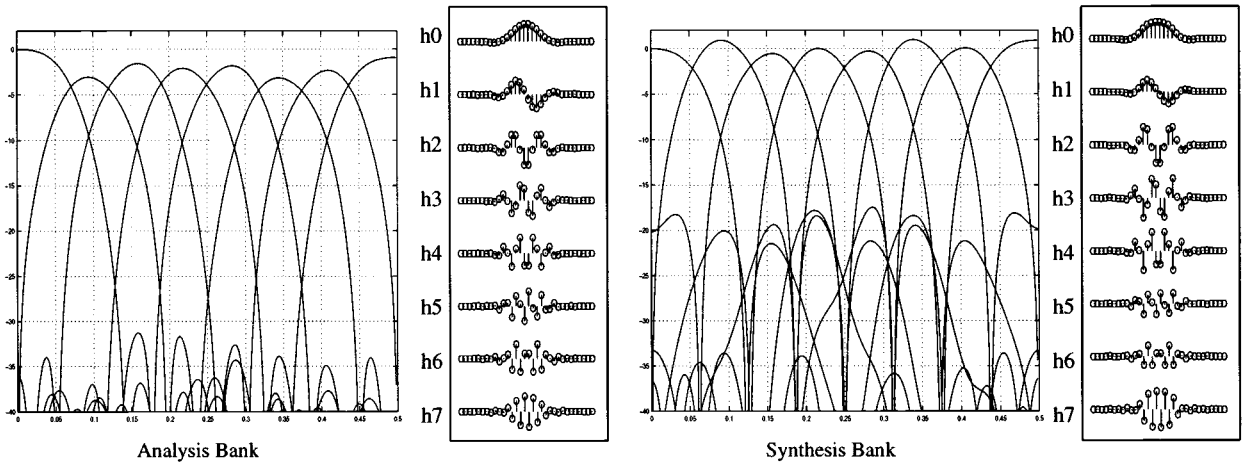

Fig. 12. Design example IV: $M = 8$ $L = 32$ optimized for stopband attenuation of analysis bank.

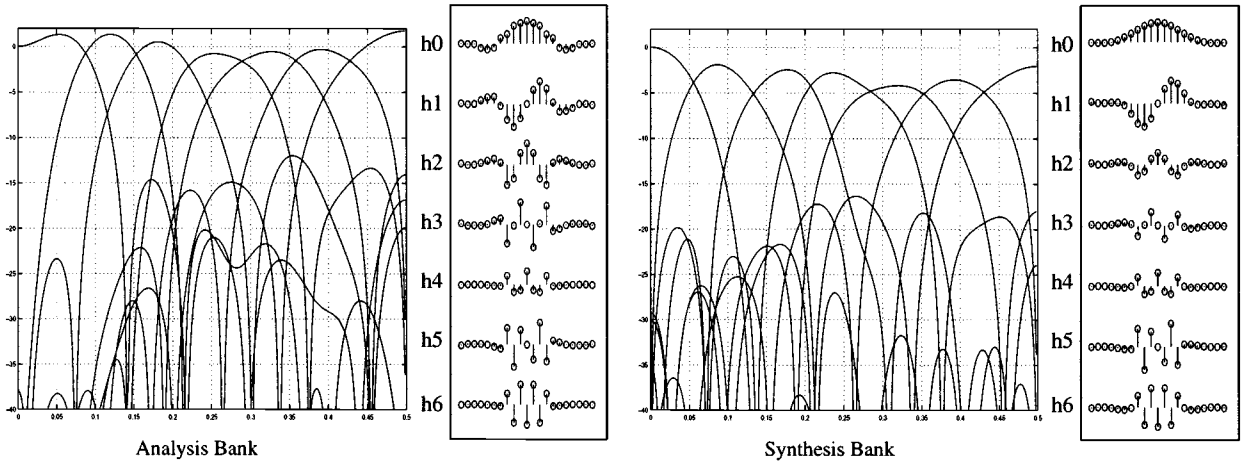

Fig. 13. Design example V: $M = 7$ $L = 21$ optimized for coding gain and stopband attenuation.

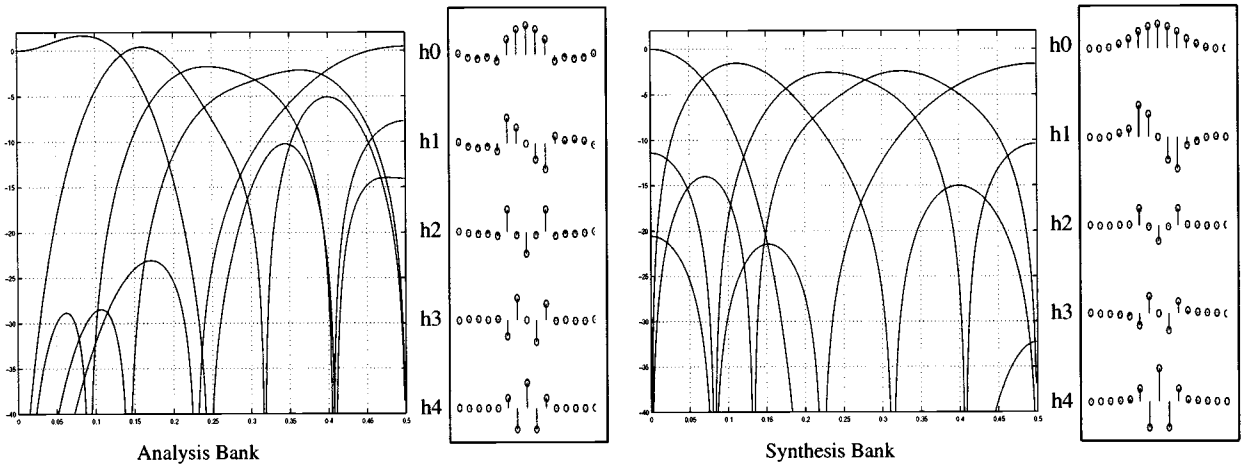

Fig. 14. Design example VI: $M = 5$ $L = 15$ optimized for coding gain and DC attenuation.

and a friendly design procedure for all LP lapped transforms with arbitrary integer overlapping factor K. In the popular even-channel case, the lattice is proven to completely span the set of all possible solutions. We also prove that the proposed lattice structures are minimal in term of the number of delays employed in its implementation for both even and odd number of channels. The relaxation of the orthogonal constraint gives the new biorthogonal LT a whole new dimension of flexibility; the analysis and the synthesis bank can now be tailored appropriately to fit a particular application. Particularly, in image coding, the analysis bank can be optimized for maximum energy compaction, whereas the synthesis filters can be designed to have a high degree of smoothness. Through the progressive image coding example, we have demonstrated

(a) (b) (c) (d)

Fig. 15. Embedded coding results of Barbara at 1 : 32 compression ratio. (a) Original image. (b) SPIHT, 27.58 dB. (c) Embedded 8 × 16 GLBT, 29.04 dB. (d) Embedded 16 × 32 GLBT, 30.18 dB.

that M-channel LPPRFB's, when appropriately designed and utilized, offer the highest performances up to date and easily surpass state-of-the-art wavelets by a significant margin.

APPENDIX
PROOF OF THEOREM II

The proof is inductive. It keys on the existence of a $\boldsymbol{G}^{-1}(z)$ matrix that reduces the order of $\boldsymbol{E}(z)$ by 1 at a time while retaining all of the desirable properties in the reduced-order $\boldsymbol{F}(z) = \boldsymbol{G}^{-1}(z)\boldsymbol{E}(z)$. The proof also serves as a guideline for the construction of the lattice given the transform coefficient matrix.

Linear Phase: Consider a stage of the lattice in Fig. 3. Note that $\boldsymbol{E}(z)$ and $\boldsymbol{F}(z)$ now have order $K-1$ and $K-2$, respectively, whereas $\boldsymbol{G}^{-1}(z)$ is anticausal with order 1. $\boldsymbol{F}(z)$ can be shown to satisfy the LP property in (4) in a similar manner to the proof of Theorem I:

$$\begin{aligned} & z^{-(K-2)}\boldsymbol{D}\boldsymbol{F}\left(z^{-1}\right)\boldsymbol{J} \\ &= z^{-(K-2)}\boldsymbol{D}\boldsymbol{G}^{-1}\left(z^{-1}\right)\boldsymbol{E}\left(z^{-1}\right)\boldsymbol{J} \\ &= z^{-(K-2)}\boldsymbol{D}\boldsymbol{G}^{-1}\left(z^{-1}\right)z^{(K-1)}\boldsymbol{D}\boldsymbol{E}(z)\boldsymbol{J}\boldsymbol{J} \\ &= z\boldsymbol{D}\boldsymbol{G}^{-1}\left(z^{-1}\right)\boldsymbol{D}\boldsymbol{G}(z)\boldsymbol{F}(z) \\ &= z\boldsymbol{D}\boldsymbol{G}^{-1}\left(z^{-1}\right)\boldsymbol{D}z^{-1}\boldsymbol{D}\boldsymbol{G}\left(z^{-1}\right)\boldsymbol{D}\boldsymbol{F}(z) = \boldsymbol{F}(z) \end{aligned}$$

where we have exploited the facts that $\boldsymbol{E}(z) = z^{-(K-1)}\boldsymbol{D}\boldsymbol{E}(z^{-1})\boldsymbol{J}$ from (1) and $\boldsymbol{G}(z) = z^{-1}\boldsymbol{D}\boldsymbol{G}(z^{-1})\boldsymbol{D}$ from Theorem I.

TABLE III
OBJECTIVE CODING RESULT COMPARISON (PSNR IN DECIBELS)

	Lena				Goldhill				Barbara			
Comp. Ratio	SPIHT 9/7 WL	8 x 40 GenLOT	8 x 16 GLBT	16 x 32 GLBT	SPIHT 9/7 WL	8 x 40 GenLOT	8 x 16 GLBT	16 x 32 GLBT	SPIHT 9/7 WL	8 x 40 GenLOT	8 x 16 GLBT	16 x 32 GLBT
1:8	40.41	40.43	40.35	40.43	36.55	36.80	36.69	36.78	36.41	38.08	37.84	38.43
1:16	37.21	37.32	37.28	37.33	33.13	33.36	33.31	33.42	31.40	33.47	33.02	33.94
1:32	34.11	34.23	34.14	34.27	30.56	30.79	30.70	30.84	27.58	29.53	29.04	30.18
1:64	31.10	31.16	31.04	31.18	28.48	28.60	28.58	28.74	24.86	26.37	26.00	27.13
1:100	29.35	29.31	29.14	29.38	27.38	27.40	27.33	27.62	23.76	24.95	24.55	25.39
1:128	28.38	28.35	28.19	28.39	26.73	26.79	26.71	26.96	23.35	24.01	23.49	24.56

Perfect Reconstruction: From (11)

$$\boldsymbol{F}(z) = \boldsymbol{G}^{-1}(z)\boldsymbol{E}(z) = \tfrac{1}{2}\boldsymbol{W}\boldsymbol{\Lambda}\left(z^{-1}\right)\boldsymbol{W}\boldsymbol{\Phi}^{-1}\boldsymbol{E}(z). \quad \text{(A.1)}$$

Since all matrices on the right-hand side of this equation have FIR inverse, $\boldsymbol{F}(z)$ is also FIR invertible, i.e., it represents an FIR perfect reconstruction system.

Causality: The above proofs for $\boldsymbol{F}(z)$ to have LP and PR are actually expected because we specifically design $\boldsymbol{G}(z)$ to propagate these properties. Any choice of $\boldsymbol{\Phi} = \left[\begin{smallmatrix}\boldsymbol{U} & \boldsymbol{0}\\ \boldsymbol{0} & \boldsymbol{V}\end{smallmatrix}\right]$ such that it is invertible will suffice. The difficult part is to show that there always exist invertible matrices $\boldsymbol{U}$ and $\boldsymbol{V}$ that will produce a causal $\boldsymbol{F}(z)$ obtained from (A.1). Let

$$\boldsymbol{F}(z) = \sum_{i=0}^{K-2} \boldsymbol{F}_i z^{-i}, \qquad \boldsymbol{F}_{K-2} \neq \boldsymbol{0}$$

and

$$\boldsymbol{E}(z) = \sum_{i=0}^{K-1} \boldsymbol{E}_i z^{-i}, \qquad \boldsymbol{E}_{K-1} \neq \boldsymbol{0}. \quad \text{(A.2)}$$

From (A.1), we have

$$\begin{aligned}\boldsymbol{F}(z) &= \tfrac{1}{2}\begin{bmatrix}\boldsymbol{I} & \boldsymbol{I}\\ \boldsymbol{I} & -\boldsymbol{I}\end{bmatrix}\begin{bmatrix}\boldsymbol{I} & \boldsymbol{0}\\ \boldsymbol{0} & z\boldsymbol{I}\end{bmatrix}\begin{bmatrix}\boldsymbol{I} & \boldsymbol{I}\\ \boldsymbol{I} & -\boldsymbol{I}\end{bmatrix}\begin{bmatrix}\boldsymbol{U}^{-1} & \boldsymbol{0}\\ \boldsymbol{0} & \boldsymbol{V}^{-1}\end{bmatrix}\boldsymbol{E}(z)\\ &= \tfrac{1}{2}\left(\begin{bmatrix}\boldsymbol{U}^{-1} & \boldsymbol{V}^{-1}\\ \boldsymbol{U}^{-1} & \boldsymbol{V}^{-1}\end{bmatrix} + z\begin{bmatrix}\boldsymbol{U}^{-1} & -\boldsymbol{V}^{-1}\\ -\boldsymbol{U}^{-1} & \boldsymbol{V}^{-1}\end{bmatrix}\right)\\ &\quad\cdot\left(\sum_{i=0}^{K-1}\boldsymbol{E}_i z^{-i}\right). \quad \text{(A.3)}\end{aligned}$$

We have to show that it is possible to eliminate the noncausal part in (A.3) by achieving

$$\begin{bmatrix}\boldsymbol{U}^{-1} & -\boldsymbol{V}^{-1}\\ -\boldsymbol{U}^{-1} & \boldsymbol{V}^{-1}\end{bmatrix}\boldsymbol{E}_0 = \boldsymbol{0}. \quad \text{(A.4)}$$

Now, let the polyphase matrix of the corresponding synthesis bank be

$$\boldsymbol{R}(z) = \sum_{i=0}^{K-1} \boldsymbol{R}_i z^{i}, \qquad \boldsymbol{R}_{K-1} \neq \boldsymbol{0} \quad \text{(A.5)}$$

where the z^{-l} factor in (1) has been absorbed into $\boldsymbol{R}(z)$ to make it anticausal. The biorthogonal condition is modified to $\boldsymbol{R}(z)\boldsymbol{E}(z) = \boldsymbol{I}$, leading to the following equivalent condition in the time domain:

$$\sum_{i=0}^{K-1-l} \boldsymbol{R}_i\boldsymbol{E}_{i+l} = \delta[l]\boldsymbol{I}, \qquad \forall l \,\text{s.t.}\, 0 \le i+l \le K-1. \quad \text{(A.6)}$$

The relationship of interest here is $\boldsymbol{R}_{K-1}\boldsymbol{E}_0 = \boldsymbol{0}$. Next, the LP property of $\boldsymbol{E}(z)$ and $\boldsymbol{R}(z)$ in (4) and (5) implies that

$$\boldsymbol{E}_i = \boldsymbol{D}\boldsymbol{E}_{K-i-1}\boldsymbol{J} \quad \text{and} \quad \boldsymbol{R}_i = \boldsymbol{J}\boldsymbol{R}_{K-i-1}\boldsymbol{D}. \quad \text{(A.7)}$$

Hence, we can obtain

$$\boldsymbol{R}_{K-1}\boldsymbol{E}_0 = \boldsymbol{J}\boldsymbol{R}_0\boldsymbol{D}\boldsymbol{E}_0 = \boldsymbol{R}_0\boldsymbol{D}\boldsymbol{E}_0 = \boldsymbol{0}.$$

Applying Sylvester's rank inequality [24] to $\boldsymbol{R}_0\boldsymbol{D}\boldsymbol{E}_0 = \boldsymbol{0}$ produces

$$\begin{aligned}&\rho(\boldsymbol{R}_0) + \rho(\boldsymbol{D}\boldsymbol{E}_0) - M \le \rho(\boldsymbol{R}_0\boldsymbol{D}\boldsymbol{E}_0) = 0\\ \Longrightarrow\quad &\rho(\boldsymbol{R}_0) + \rho(\boldsymbol{E}_0) \le M. \quad \text{(A.8)}\end{aligned}$$

The proof of causality is accomplished if $\rho(\boldsymbol{E}_0) \le M/2$ since in that case, the dimension of the null space of $\boldsymbol{E}_0$ is larger than or equal to $M/2$. Hence, it is possible to choose $M/2$ linearly independent vectors from $\boldsymbol{E}_0$'s null space to serve as $[\boldsymbol{U}^{-1} - \boldsymbol{V}^{-1}]$. In the paraunitary case, this can be achieved easily because (3) immediately implies $\rho(\boldsymbol{R}_0) = \rho(\boldsymbol{E}_0) \le M/2$. The biorthogonal case is more troublesome, and we need the following Lemma I, which shows that the condition $\rho(\boldsymbol{E}_0) > M/2$ [or $\rho(\boldsymbol{R}_0) > M/2$] leads to asymmetrical systems where the filters of one bank have higher order than the filters of the other. More simply stated, in the case where all analysis and synthesis filters have linear phase and the same length $L = KM$, it is necessary that

$$\rho(\boldsymbol{E}_0) \le \frac{M}{2} \quad \text{and} \quad \rho(\boldsymbol{R}_0) \le \frac{M}{2}.$$

Order Reduction: It can be easily verified that the structure $\boldsymbol{G}^{-1}(z)$ in (A.1) with $\boldsymbol{U}$ and $\boldsymbol{V}$ chosen to eliminate noncausality as in (A.4) also reduces the order of $\boldsymbol{E}(z)$ by 1. From (A.3), after one factorization step, the highest order component of $\boldsymbol{F}(z) = \boldsymbol{G}^{-1}(z)\boldsymbol{E}(z)$ is

$$\begin{bmatrix}\boldsymbol{U}^{-1} & \boldsymbol{V}^{-1}\\ \boldsymbol{U}^{-1} & \boldsymbol{V}^{-1}\end{bmatrix}\boldsymbol{E}_{K-1}. \quad \text{(A.9)}$$

Substituting $\boldsymbol{E}_{K-1} = \boldsymbol{D}\boldsymbol{E}_0\boldsymbol{J}$ from (A.7) into (A.9) yields

$$\begin{bmatrix} \boldsymbol{U}^{-1} & \boldsymbol{V}^{-1} \\ \boldsymbol{U}^{-1} & \boldsymbol{V}^{-1} \end{bmatrix} \boldsymbol{D}\boldsymbol{E}_0\boldsymbol{J} = \begin{bmatrix} \boldsymbol{U}^{-1} & -\boldsymbol{V}^{-1} \\ \boldsymbol{U}^{-1} & -\boldsymbol{V}^{-1} \end{bmatrix} \boldsymbol{E}_0\boldsymbol{J} = \boldsymbol{0}\boldsymbol{J} = \boldsymbol{0}. \tag{A.10}$$

Therefore, the factorization is guaranteed to terminate after $(K-1)$ steps. □

Lemma I: If there exist two polyphase matrices $\boldsymbol{E}(z) = \sum_{i=0}^{K-1} \boldsymbol{E}_i z^{-i}$ and $\boldsymbol{R}(z) = \sum_{i=0}^{K-1} \boldsymbol{R}_i z^{i}$ representing FIR even-channel LPPRFB with all filters having the same length $L = KM$, then $\rho(\boldsymbol{E}_0) \leq M/2$, and $\rho(\boldsymbol{R}_0) \leq M/2$.

Proof: Note that we consider the causal analysis bank and the anticausal synthesis bank purely for the clarity of presentation. Equation (1) now simplifies to $\boldsymbol{R}(z)\boldsymbol{E}(z) = \boldsymbol{I}$, whereas $|\boldsymbol{E}(z)| = z^{-m} = 1/|\boldsymbol{R}(z)|$ and $|\boldsymbol{R}(z)| = z^{m}$. Indeed, we can manipulate (4) and (5) in similar fashions to the techniques in the proof of Theorem III to obtain the exact order m of their determinants:

$$\begin{aligned} |\boldsymbol{E}(z)| &= \left|z^{-(K-1)}\boldsymbol{I}\right| |\boldsymbol{D}| \left|\boldsymbol{E}\left(z^{-1}\right)\right| |\boldsymbol{J}| \\ &= z^{-M(K-1)} \frac{1}{|\boldsymbol{E}(z)|} \\ \Longrightarrow\ |\boldsymbol{E}(z)| &= z^{-(M(K-1)/2)}. \end{aligned}$$

We will complete the proof by contradiction. Suppose that $\rho(\boldsymbol{E}_0) > M/2$; thus, $\rho(\boldsymbol{R}_0) < M/2$. Consider the possibility of the factorization of the anticausal $\boldsymbol{R}(z)$. Similarly to the approach described by (A.3) and (A.4), we need to obtain

$$\boldsymbol{R}_0 \begin{bmatrix} \boldsymbol{U} & -\boldsymbol{U} \\ -\boldsymbol{V} & \boldsymbol{V} \end{bmatrix} = \boldsymbol{0} \tag{A.11}$$

to eliminate causality. In this case, $\rho(\boldsymbol{R}_0) < M/2$, and it is possible to choose $[\boldsymbol{U} \quad -\boldsymbol{V}]^T$ from $M/2$ linearly independent vectors from the null space of $\boldsymbol{R}_0$. In other words, it is possible to write $\boldsymbol{R}(z)$ as $\boldsymbol{R}(z) = \boldsymbol{R}_{K-2}(z)\boldsymbol{G}^{-1}(z)$, where both factors are anticausal. Now, $|\boldsymbol{R}(z)| = |\boldsymbol{R}_{K-2}(z)||\boldsymbol{G}^{-1}(z)|$. Since $|\boldsymbol{G}^{-1}(z)| = z^{M/2}$, $|\boldsymbol{R}_{K-2}(z)| = z^{(M(K-1)/2)-(M/2)} = z^{(M(K-2))/2}$. Therefore, it is easy to show that $\boldsymbol{R}_{K-2}(z)$ represents an FIR LPPR system of order $(K-2)$.

On the other hand, $\boldsymbol{E}(z) = \boldsymbol{R}^{-1}(z) = \boldsymbol{G}(z)\boldsymbol{R}_{K-2}^{-1}(z)$. Consider the product $\boldsymbol{G}^{-1}(z)\boldsymbol{E}(z) = \boldsymbol{R}_{K-2}^{-1}(z)$. We have $\boldsymbol{R}_{K-2}^{-1}(z)$ causal with determinant $z^{-(M(K-2)/2)}$. However, since $\rho(\boldsymbol{E}_0) > M/2$, the null space of $\boldsymbol{E}_0$ has dimension less than $M/2$. Therefore, the anticausal part of $\boldsymbol{G}^{-1}(z)\boldsymbol{E}(z)$ cannot possibly be suppressed, i.e.,

$$\begin{bmatrix} \boldsymbol{U}^{-1} & -\boldsymbol{V}^{-1} \\ -\boldsymbol{U}^{-1} & \boldsymbol{V}^{-1} \end{bmatrix} \boldsymbol{E}_0 \neq \boldsymbol{0}$$

for any invertible matrices $\boldsymbol{U}^{-1}$ and $\boldsymbol{V}^{-1}$. Moreover, the highest order of $\boldsymbol{G}^{-1}(z)\boldsymbol{E}(z)$ still exists as

$$\begin{bmatrix} \boldsymbol{U}^{-1} & \boldsymbol{V}^{-1} \\ \boldsymbol{U}^{-1} & \boldsymbol{V}^{-1} \end{bmatrix} \boldsymbol{E}_{K-1} \neq \boldsymbol{0}$$

because $\rho(\boldsymbol{E}_{K-1}) = \rho(\boldsymbol{E}_0) > M/2$. Theefore, , a shift of z leads to a causal system with order K, which is contradictory to the fact that $\boldsymbol{R}_{K-2}^{-1}(z)$ is causal with order $(K-2)$. The case of $\rho(\boldsymbol{R}_0) > M/2$ can be proven in a similar fashion. □

REFERENCES

[1] P. P. Vaidyanathan, *Multirate Systems and Filter Banks*. Englewood Cliffs, NJ: Prentice-Hall, 1993.

[2] G. Strang and T. Q. Nguyen, *Wavelets and Filter Banks*. Wellesley, MA: Wellesley-Cambridge, 1996.

[3] M. Vetterli and J. Kovačević, *Wavelets and Subband Coding*. Englewood Cliffs, NJ: Prentice-Hall, 1995.

[4] A. K. Soman, P. P. Vaidyanathan, and T. Q. Nguyen, "Linear-phase paraunitary filter banks: Theory, factorizations and applications," *IEEE Trans. Signal Processing*, vol. 41, pp. 3480–3496, Dec. 1993.

[5] R. L. de Queiroz, T. Q. Nguyen, and K. R. Rao, "The GenLOT: Generalized linear-phase lapped orthogonal transform," *IEEE Trans. Signal Processing*, vol. 40, pp. 497–507, Mar. 1996.

[6] T. D. Tran and T. Q. Nguyen, "On M-channel linear-phase FIR filter banks and application in image compression," *IEEE Trans. Signal Processing*, vol. 45, pp. 2175–2187, Sept. 1997.

[7] T. D. Tran, M. Ikehara, and T. Q. Nguyen, "Linear phase paraunitary filter bank with filters of different lengths and its application in image compression," IEEE Trans. Signal Processing, to be published.

[8] T. Q. Nguyen and P. P. Vaidyanathan, "Two channel PR FIR QMF structures which yield linear-phase analysis and synthesis filters," *IEEE Trans. Acoust., Speech, Signal Processing*, vol. 37, pp. 676–690, May 1989.

[9] M. Vetterli and D. Le Gall, "Perfect-reconstruction filter banks: Some properties and factorizations," *IEEE Trans. Acoust., Speech, Signal Processing*, vol. 37, pp. 1057–1071, July 1989.

[10] H. Kiya, M. Yae, and M. Iwahashi, "A linear-phase two-channel filter bank allowing perfect reconstruction," in *Proc. IEEE Int. Symp. Circuits Syst.*, San Diego, CA, May 1992, pp. 951–954.

[11] M. Vetterli and C. Herley, "Wavelets and filter banks: Theory and design," *IEEE Trans. Signal Processing*, vol. 40, pp. 2207–2232, Sept. 1992.

[12] T. Q. Nguyen, "Digital filter banks design—Quadratic-constrained formulation," *IEEE Trans. Signal Processing*, vol. 43, pp. 2103–2108, Sept. 1995.

[13] K. Nayebi, T. Barnwell, and M. J. Smith, "Time-domain filter bank analysis: A new design theory," *IEEE Trans. Signal Processing*, vol. 40, pp. 1412–1429, June 1992.

[14] P. Saghizadeh and A. N. Willson, Jr., "A generic approach to the design of M-channel uniform-band perfect-reconstruction linear phase FIR filter banks," in *Proc. IEEE Int. Conf. Acoust., Speech, Signal Process.*, Detroit, MI, May 1995, pp. 1300–1303.

[15] Y. P. Lin and P. P. Vaidyanathan, "Linear phase cosine modulated maximally decimated filter banks with perfect reconstruction," *IEEE Trans. Signal Processing*, pp. 2525–2539, Nov. 1995.

[16] S. C. Chan, "The generalized lapped transform (GLT) for subband coding applications," in *Proc. IEEE Int. Conf. Acoust., Speech, Signal Process.*, Detroit, MI, May 1995, pp. 1508–1511.

[17] H. S. Malvar, "Lapped biorthogonal transforms for transform coding with reduced blocking and ringing artifacts," in *Proc. IEEE Int. Conf. Acoust., Speech, Signal Process.*, Munich, Apr. 1997.

[18] H. S. Malvar, "Biorthogonal and nonuniform lapped transforms for transform coding with reduced blocking and ringing artifacts," *IEEE Trans. Signal Processing*, vol. 46, pp. 1043–1053, Apr. 1998.

[19] ——, *Signal Processing with Lapped Transforms*. Norwood, MA: Artech House, 1992.

[20] K. R. Rao and P. Yip, *Discrete Cosine Transform: Algorithms, Advantages, Applications*. New York: Academic, 1990.

[21] A. Said and W. A. Pearlman, "A new fast and efficient image codec based on set partitioning in hierarchical trees," *IEEE Trans. Circuits Syst. Video Technol.*, vol. 6, pp. 243–250, June 1996.

[22] S. Basu and H. M. Choi, "Hermite-like reduction method for linear-phase perfect reconstruction filter bank design," in *Proc. IEEE Int. Conf. Acoust, Speech, Signal Process*, Detroit, MI, May 1995, pp. 1512–1515.

[23] E. Kofidis, S. Theodoridis, and N. Kaloupsidis, "On the perfect reconstruction problem in N band multirate maximally decimated FIR filter banks," *IEEE Trans. Signal Processing*, vol. 44, pp. 2439–2455, Oct. 1996.

[24] F. R. Gantmacher, *The Theory of Matrices*, New York: Chelsea, 1977.

[25] P. P. Vaidyanathan and T. Chen, "Role of anticausal inverses in multirate filter banks—Part I: System-theoretic fundamentals," *IEEE Trans. Signal Processing*, vol. 43, pp. 1090–1102, May 1995.

[26] C. W. Kok, T. Nagai, M. Ikehara, and T. Q. Nguyen, "Structures and factorization of linear phase paraunitary filter banks," in *Proc. IEEE Int. Symp. Circuits Syst.*, Hong Kong, June 1997.

[27] R. A. Horn and C. R. Johnson, *Matrix Analysis*. Cambridge, U.K.: Cambridge Univ. Press, 1985.
[28] P. P. Vaidyanathan and T. Chen, "Role of anticausal inverses in multirate filter banks—Part II: The FIR case, factorizations, and biorthogonal lapped transforms," *IEEE Trans. Signal Processing*, vol. 43, pp. 1103–1115, May 1995.
[29] T. A. Ramstad, S. O. Aase, and J. H. Husoy, *Subband Compression of Images: Principles and Examples*. New York: Elsevier, 1995.
[30] J. Katto and Y. Yasuda, "Performance evaluation of subband coding and optimization of its filter coefficients," in *SPIE Proc. Visual Commun. Image Process.*, Boston, MA, Nov. 1991, pp. 95–106.
[31] S. O. Aase and T. A. Ramstad, "On the optimality of nonunitary filter banks in subband coders," *IEEE Trans. Image Processing*, vol. 4, pp. 1585–1591, Dec. 1995.
[32] T. D. Tran and T. Q. Nguyen, "A progressive transmission image coder using linear phase filter banks as block transforms," , submitted for publication.
[33] ——, "A progressive transmission image coder using linear phase paraunitary filter banks," in *Proc. 31st Asilomar Conf. SSC*, Pacific Grove, CA, Nov. 1997.

Trac D. Tran received the B.S. and M.S. degrees from the Massachusetts Institute of Technology, Cambridge, in 1994 and the Ph.D. degree from the University of Wisconsin, Madison, in 1998, all in electrical engineering.

He joined the Department of Electrical and Computer Engineering, The Johns Hopkins University, Baltimore, MD, in July 1998 as an Assistant Professor. His research interests are in the field of digital signal processing, particularly in multirate systems, filter banks, transforms, wavelets, and their applications in signal analysis, compression, processing, and communications.

Dr. Tran was the codirector (with Prof. J. L. Prince) of the 33rd Annual Conference on Information Sciences and Systems (CISS'99), Baltimore, MD, in March 1999. He is a member of Eta Kappa Nu and Tau Beta Pi.

Ricardo L. de Queiroz (SM'99) received the B.S. degree from Universidade de Brasilia, Brasilia, Brazil, in 1987, the M.S. degree from Universidade Estadual de Campinas, Campinas, Brazil, in 1990, and the Ph.D. degree from the University of Texas, Arlington (UTA), in 1994, all in electrical engineering.

From 1990 to 1991, he was with the DSP Research Group at Universidade de Brasilia as a Research Associate. In 1994, he was a Teaching Assistant at UTA. He joined Xerox Corporation, Webster, NY, in August 1994, where he is currently a member of the research staff at the Color and Digital Imaging Systems Lab Group. His research interests are multirate signal processing, image and signal compression, color imaging, and processing compressed images. He has contributed chapters to books, published extensively in journals and conferences, and holds a number of patents.

Dr. de Quiroz is an Associate Editor for the IEEE SIGNAL PROCESSING LETTERS and is currently serving as Chair of the Rochester Chapter of the IEEE Signal Processing Society. In 1993, he received the Academic Excellence Award from the Electrical Engineering Department of UTA. He is a member of IS&T.

Truong Q. Nguyen (S'85–M'90–SM'95) received the B.S., M.S., and Ph.D. degrees in electrical engineering from the California Institute of Technology, Pasadena, in 1985, 1986, and 1989, respectively.

He was with the Massachusetts Institute of Technology (MIT) Lincoln Laboratory, Lexington, from June 1989 to July 1994, as a Member of the Technical Staff. From 1993 to 1994, he was a Visiting Lecturer at MIT and an Adjunct Professor at Northeastern University, Boston, MA. From August 1994 to July 1996, he was an Assistant and Associate Professor at the University of Wisconsin, Madison. He is now with Boston University, Boston, MA. His research interests are in digital and image signal processing, multirate systems, wavelets and applications, and biomedical signal processing.

Prof. Nguyen was a recipient of a fellowship from Aerojet Dynamics for advanced studies. He received the IEEE TRANSACTIONS IN SIGNAL PROCESSING Paper Award (image and multidimensional processing area) for the paper he cowrote with Prof. P. P. Vaidyanathan on linear-phase perfect-reconstruction filter banks in 1992. He received the NSF Career Award in 1995 and is the coauthor (with Prof. G. Strang) of a textbook on *Wavelets and Filter Banks* (Wellesley, MA: Wellesley-Cambridge). He was an Associate Editor for the IEEE TRANSACTIONS ON SIGNAL PROCESSING and for the IEEE TRANSACTIONS ON CIRCUITS AND SYSTEMS II and has also served on the Digital Signal Processing Technical Committee for the IEEE Circuits and Systems Society. He is a member of Tau Beta Pi and Eta Kappa Nu.